Report 3325

NAVAL SHIP RESEARCH AND DEVELOPMENT CENTER
Washington, D.C. 20007

MODEL AND PROTOTYPE RESPONSES FOR A DL CLASS DESTROYER

by
John N. Andrews

DEPARTMENT OF STRUCTURAL MECHANICS
RESEARCH AND DEVELOPMENT REPORT

March 1970

Report 3325

MODEL AND PROTOTYPE RESPONSES FOR A DL CLASS DESTROYER

The Naval Ship Research and Development Center is a U.S. Navy center for laboratory effort directed at achieving improved sea and air vehicles. It was formed in March 1967 by merging the David Taylor Model Basin at Carderock, Maryland and the Marine Engineering Laboratory at Annapolis, Maryland. The Mine Defense Laboratory, Panama City, Florida became part of the Center in November 1967.

Naval Ship Research and Development Center
Washington, D.C. 20007

NDW-NSRDC 3960/43 (10-67)

DEPARTMENT OF THE NAVY
NAVAL SHIP RESEARCH AND DEVELOPMENT CENTER
WASHINGTON, D. C. 20007

MODEL AND PROTOTYPE RESPONSES FOR A DL CLASS DESTROYER

by

John N. Andrews

March 1970 Report 3325

TABLE OF CONTENTS

LIST OF FIGURES

Page

Page

Page

LIST OF TABLES

NOTATION

B	Ship beam (49 ft, 9 1/4 in.)
E	Area under spectrum
L_s	Ship length between perpendiculars (476 ft)
ρg	Weight density of sea water (64 lb/ft^3)
ω_e	Encounter frequency
ω_L	Frequency of wave equal to ship length, $\sqrt{2\pi g/L_s}$
ω_w	Wave frequency
Ω_e	Nondimensional encounter frequency, ω_e/ω_L
Ω_w	Nondimensional wave frequency, ω_w/ω_L

ABSTRACT

This report presents test results for a segmented structural model of the DL-2-Class destroyer in random waves (unidirectional and bidirectional) together with regular wave results derived from earlier tests. Vertical and transverse bending moments were measured at two longitudinal positions on the model. Vertical and transverse shear forces were measured at the quarter-point. Motion measurements (pitch angle, roll angle, bow acceleration, and heave displacement) were made as were pressures at two positions along the keel.

Response amplitude operators (RAOs) derived from regular and random wave tests are compared. Neumann sea spectra, together with the RAOs, are utilized to obtain prediction curves of ship response. Maximum whipping response for the vertical midship bending moment is augmented with the maximum wave-induced response and compared with the conventional design midship bending moment. The spectra for two unidirectional seas whose directions are 90 deg apart were combined and compared with the corresponding bidirectional sea. The same procedure was applied to the corresponding midship vertical bending moment response.

Comparison of model and prototype test results are made by means of prediction curves.

ADMINISTRATIVE INFORMATION

The experimental investigation of the response of slender, high-speed displacement ships in waves was originally carried out as part of the in-house independent research program of the Naval Ship Research and Development Center. The work reported herein was authorized by Naval Ship Engineering Center (NAVSEC) letter F-013 0301 Serial 442-202 of 11 October 1963 and was funded by (NAVSHIP) under Task 1973 of Task Area S-F 35-422 301.

INTRODUCTION

This report is an extension of a previously reported work[1] which presented regular wave test results for a segmented structural model of a DL-2-Class destroyer. This report compares the results of the earlier

---

[1]References are listed on page 54.

tests with those obtained in random waves, compares the experimental results with conventional design criteria, and compares model and prototype test results.

METHOD

MODEL AND TEST PROGRAM

The 20-ft-long model (scale ratio = 23.8) was constructed to conform to the lines of a DL-2-Class destroyer and was segmented at seven longitudinal locations. Detailed descriptions of the model and the instrumentation employed to record the measurements are available in Reference 1. The applicable scaling laws are based on the well-known Froude principle. The general properties of the model are given in Table 1 in terms of the prototype values. Figure 1 depicts the general arrangement of the model, and Figure 2 is a profile of the prototype ship.

The model was self-propelled and tested in the MASK facility at this Center in both unidirectional and bidirectional random waves at various headings and at a ship speed of 5 knots. Table 2 is a schedule of tests performed in random waves. Because of the size limitation of the basin, between three and five test runs (depending on heading) were required for each random wave condition in order to obtain equivalent full-scale test runs of 20-min intervals. This test period was considered necessary to adequately describe the wave and response characteristics via spectral analysis.

MEASUREMENTS

Vertical and transverse bending moments were measured at Station 5 (quarter-point) and Station 10 (amidships). Vertical and transverse shear forces were measured at Station 5. Motions (pitch angle, roll angle, bow acceleration, and heave displacement) as well as pressures along the keel at Station 5 and Station 10 were also measured. The motion and pressure measurements reported here are for one test condition only, namely with the model running in a quarter-head sea. Structural measurements were obtained during the test conditions described in Table 2.

ANALYSIS

Spectral analysis was employed to derive response characteristics of the model. Briefly, a spectrum of a random process is a frequency decomposition of the process and a plot of the mean-squared value of the process per unit of frequency versus frequency.

One of the most important properties of a spectrum[2] is that the area (E) it encloses may be employed to estimate maximum peak-to-peak variations of the process.* The most useful aspect of spectral analysis is in the determination of the response amplitude operators (RAOs) which characterize response from a knowledge of the excitation and response spectra. An RAO is a plot of the square of response per unit of excitation versus frequency.

To directly compare model and prototype results or to compare them to other ships, it is advantageous to nondimensionalize the RAOs as shown herein. Although RAOs are useful in defining ship response characteristics, it should be emphasized that they are valid only for the ordinary wave-induced responses, exclusive of vibratory (whipping) responses which by nature are transient. Accordingly, to obtain the RAO for wave-induced response, the response records were filtered to remove the vibratory components.

RAOs obtained from the experiments were then employed together with theoretical Neumann sea spectra to obtain prediction curves of ship responses. The prediction curves were then utilized to obtain the effect of ship heading on response.

Maximum whipping response of the structural measurements were recorded. The maximum whipping response for the midship vertical bending moment was augmented with the maximum wave-induced response for comparison with the conventional design midship bending moment.

---

* 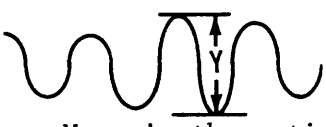

$$Y_{max} = 2\sqrt{E \log_e N}$$

where Y_{max} is the estimated peak-to-peak (double amplitude) variation of the process and N is the total number of peak-to-peak variations in the process.

PRESENTATION AND DISCUSSION OF RESULTS

Figures 3 through 5 respectively show the $\sqrt{RAO}$ plots for midship vertical bending moment, for Station 5 vertical bending moment, and for Station 5 vertical shear force with the model running into head seas. Three sea conditions corresponding to States 4, 6, and 7 seas were generated to determine the effect of sea severity on the RAO amplitudes. It is evident from the figures that severity of the sea had little effect on the magnitudes of the RAO for the conditions cited here. Accordingly, average values of the RAOs are utilized in succeeding presentations where several sea conditions are given for the same heading. In each figure mentioned above as well as in succeeding figures, the $\sqrt{RAO}$ values are given in terms of nondimensional values and in terms of prototype values. Also along the abscissa, the frequency is given in terms of prototype values. Also along the abscissa, the frequency is given in terms of nondimensional values for both encounter and wave frequency.

Figures 6 through 38 are plots of $\sqrt{RAOs}$ for the tests conducted in unidirectional seas. Some of these figures also include $\sqrt{RAO}$ plots for tests conducted earlier in regular waves.[1] Only those regular wave tests that correspond in heading to the unidirectional random wave tests are given on the figures. Figures 6, 11, and 16 show the average values of the RAOs depicted in Figures 3 through 5. The $\sqrt{RAO}$ magnitudes of the random wave test results were faired at the ends in accordance with procedures described in Reference 1 in order to be consistent with the regular wave test results. The agreement of random and regular wave results is quite evident from a comparison of the above-mentioned figures. Even where little response would be expected, e.g., in such cases as vertical response in beam waves and transverse response in head seas, the correlation between random and regular wave results is apparent.

Figures 39 through 50 are plots of $\sqrt{RAO}$ magnitudes obtained from bidirectional wave tests. Comparison of these plots with the corresponding plots for the unidirectional tests again indicates good agreement.

The plots of ship response for unidirectional waves shown in Figures 51-65 were obtained by multiplying the RAO magnitudes by the

Neumann sea spectra for various wind speeds to produce response spectra. The areas E under the response spectra were determined and the $\sqrt{E}$ values then plotted. In the cases where both random and regular wave results are shown, the agreement is excellent. This is expected of course since the $\sqrt{RAO}$ magnitudes for both the random and regular wave results discussed previously showed good correlation. Each figure contains experimental points which are the root-mean-squared (rms) values obtained from the area of the spectra generated in the tank. In general, the wave spectra were generated so that the peak value in each wave spectra would coincide with the nondimensional wave frequency (Ω_W) equal to one, and the wave amplitudes were varied according to severity of sea state desired based on the Neumann sea spectra. The degree to which the energy contained in the Neumann spectra was produced is found by comparing on the figures the rms experimental values with the nearest rms values on the curves. In most cases, the experimental points lie near or on the prediction curves. Table 3 lists the experimental rms values for both wave and structural response results obtained during the model tests. Experimental rms values obtained for the motion and pressure responses in a State 6 sea with the model running 45 deg into the waves are listed below:

Wave amplitude	4.57 ft
Pitch angle	1.44 deg
Roll angle	4.81 deg
Heave displacement	2.93 ft
Bow acceleration	0.133 g
Pressure at Station 5	128.8 lb/ft^2
Pressure at Station 10	66.7 lb/ft^2

The effect of ship heading is evident from the figures. For vertical ship response, there is an attenuation in magnitude as headings progress to beam waves and an increase in amplitude for transverse response.

Figures 66-71 show another means of demonstrating the effect of ship heading on response. The prediction curves were utilized in constructing these plots, and the response magnitudes corresponding to specific rms wave amplitudes were read for each available heading. These figures clearly show that maximum vertical ship response is to be expected in head or near head seas whereas maximum transverse ship response occurs somewhere between headings of 45 and 60 deg.

Figures 72 through 77 are plots of prediction curves for ship response in bidirectional waves. These are quite similar to the corresponding prediction curves derived from unidirectional wave results. This was as expected since there was good agreement between the unidirectional and bidirectional $\sqrt{RAO}$ magnitudes.

To determine the validity of the superposition[3] of different unidirectional wave conditions, the energies of the different wave conditions were added and the combined result was compared to a bidirectional wave condition. The result is demonstrated in Figure 78 where the wave spectral density for the State 6 sea of Case 1 (see Table 2) has been added to the wave spectral density of Case 5. Also shown in the figure is the wave spectrum for Case 6 which is a bidirectional wave condition. When this wave condition was generated, the same wavemaking program that was utilized to generate the unidirectional wave spectra for each bank was employed simultaneously for each respective bank. The comparison of the curves is quite good. The response spectra corresponding to the wave conditions of Figure 78 for midship vertical moment were employed as an example of the superposition of responses. The results (Figure 79) indicate that here again, correlation is excellent. If the E values are compared, the error is found to be less than 3 percent.

The sum of the maximum wave-induced midship vertical bending and whipping moment values in terms of double amplitudes (peak-to-peak) is shown in Figure 80 by the solid line extended by dashes. This curve was obtained from the recorded data listed in Table 4 which indicates the maximum structural responses obtained from the test data. The complete dashed line is similar to the experimental line except that the maximum wave-induced values were derived using the formula given in the footnote to page 3 of this report. The whipping values used to construct this line were obtained from the curve for whipping response shown in the figure. The extension of the lines by straight lines is based on the partial evidence presented here, i.e., the three experimental points lie along a straight line, and from other investigations.[4,5] In addition to the above-mentioned lines, the figure shows a straight horizontal line representing the special hog to sag design moment (229, 600 ft-tons) for the prototype ship. The intersection of the design moment line with the

experimental line occurs in a high State 7 sea whereas the prediction curve intersects the design moment line in a low State 7 sea; hence it produces a more conservative result. This result has also been determined from tests conducted aboard the full-scale ship.[6] It should be emphasized here that the whipping responses presented were obtained with the model running at a ship speed of 5 knots. Other investigations[4,5] have shown that the whipping response increases greatly with ship speed as well as with wave height as demonstrated herein. Thus since a State 7 sea is realizable, Figure 80 indicates that the integrity of the ship hull girder may be doubtful if such a sea condition is encountered during a ship mission.[7] Certainly high speeds are to be avoided during encounters with such seas.

PROTOTYPE AND MODEL COMPARISONS

To this point, the present report has been concerned with comparisons of model response in random and regular waves. No matter how good such correlations may be, they mean little if the methods do not predict prototype results. Therefore this section will compare the responses predicted by model studies to those actually measured during sea trials.

The DL-2-Class destroyer was picked for this program because a full-scale evaluation program was underway on one of the DL-2-Class ships, the USS WILLIS A. LEE (DL-4) and could provide the full-scale response data necessary to check the model prediction. The model and full-scale tests were coordinated so that speed was essentially the same (model and prototype). Since most of the prototype tests were run in confused (bidirectional) seas, the model results used for comparison were data from the bidirectional random seas.

Sufficient data are available to compare model and prototype responses as follows:

Bow Pressure	Head Sea
Pitch Angle	Head Sea
Vertical Bending	Quarter-Head Sea
Roll	Beam Sea

The comparisons are shown in Figures 81-85. In general the results are quite good, particularly for pitch and roll. The greatest discrepancy

found was that for head sea vertical bending. This is to be expected since the wave recorder used to determine prototype sea states may indicate waves as much as 10 percent higher than they really are. Also the ship superstructure does carry some load which is not considered in the model. Even with these errors, however, the model predictions are good enough to be used to predict full-scale response.

CONCLUSIONS

The purpose of this report was to compare the results of tests run in regular waves with those run in random waves. Because tests can be run in random waves far quicker and cheaper than in regular waves, they would therefore be more desirable for future tests if their results were similar to those obtained in regular waves. On the basis of the experiments conducted, it appears that:

1. The prediction curves and the square root of the response amplitude operators are substantially the same for regular and random waves and therefore more widespread use of the cheaper random test program is possible.

2. Superposition of several unidirectional random wave conditions may be used to produce a bidirectional wave condition.

3. The severity of the waves has little effect on the magnitude of $\sqrt{RAO}$.

4. Whipping stresses must be considered in the design of the hull girder since these are superimposed on the ordinary wave-induced responses and in severe seas (States 6 to 7) are as much as the ordinary wave-induced responses.

5. There is good agreement between results from these model tests and those obtained from full-scale trials of WILLIS A. LEE.

ACKNOWLEDGMENT

The author gratefully acknowledges the assistance of Mr. A.L. Dinsenbacher, Vibration Division of the Department of Acoustics and Vibration, who was primarily responsible for the development of the model program.

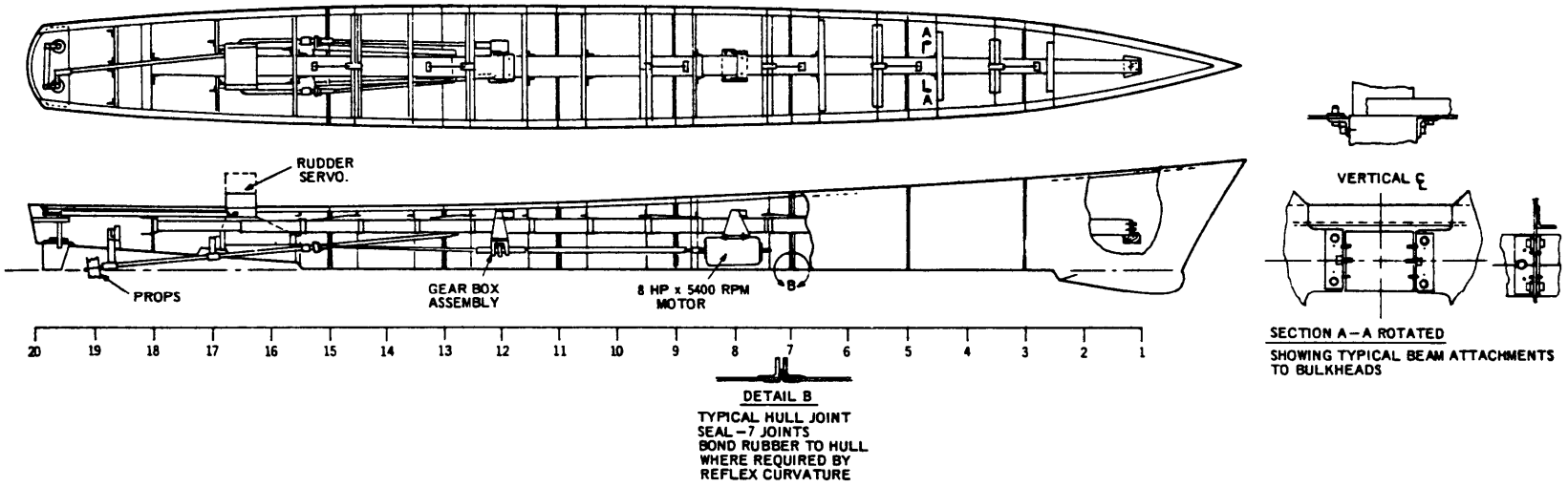

Figure 1 - Model of DL-2-Class Destroyer

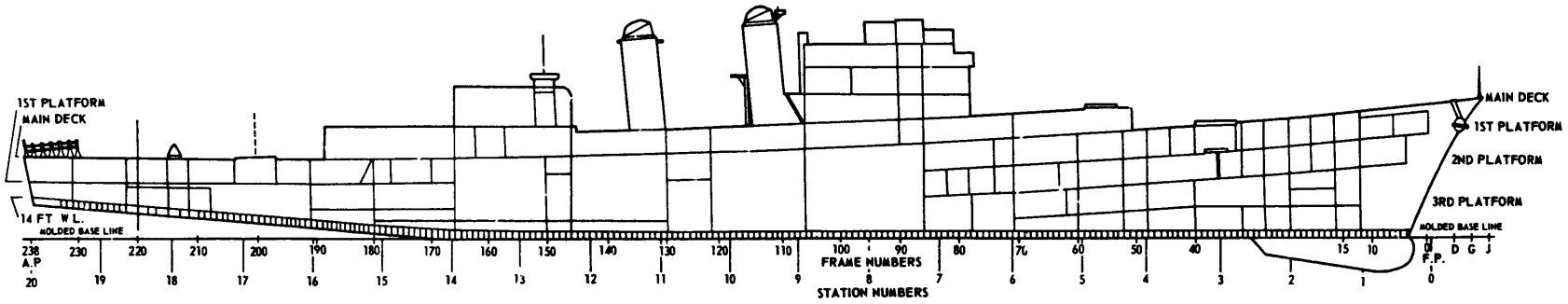

Figure 2 - DL-2-Class Destroyer

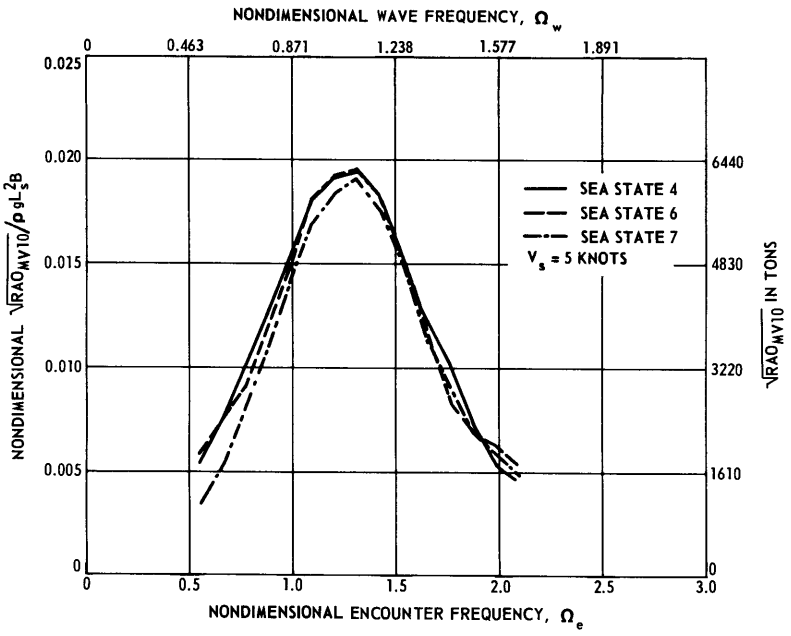

Figure 3 - Root of Midship Vertical Bending Moment RAO, Heading Zero

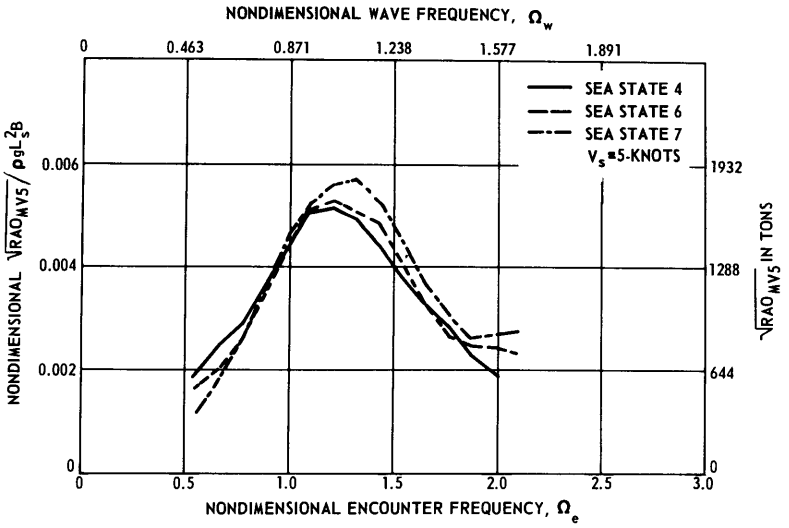

Figure 4 - Root of Station 5 Vertical Bending Moment RAO, Heading Zero

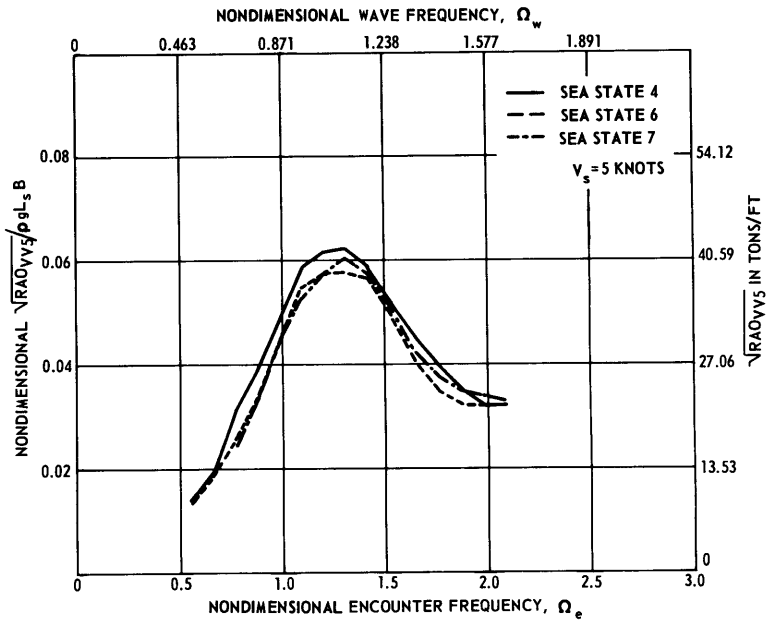

Figure 5 - Root of Station 5 Vertical Shear RAO
Heading Zero

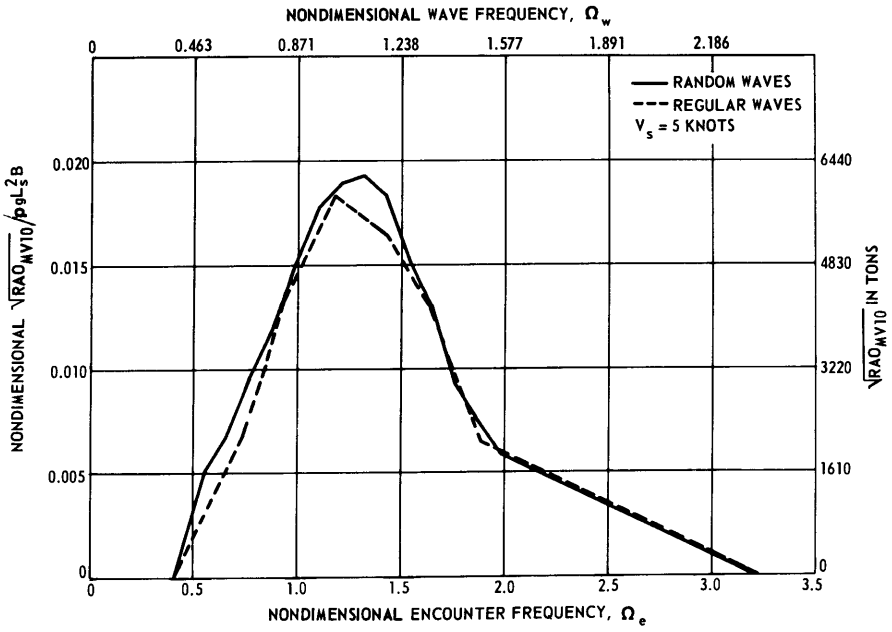

Figure 6 - Root of Midship Vertical Bending Moment RAO,
Heading Zero

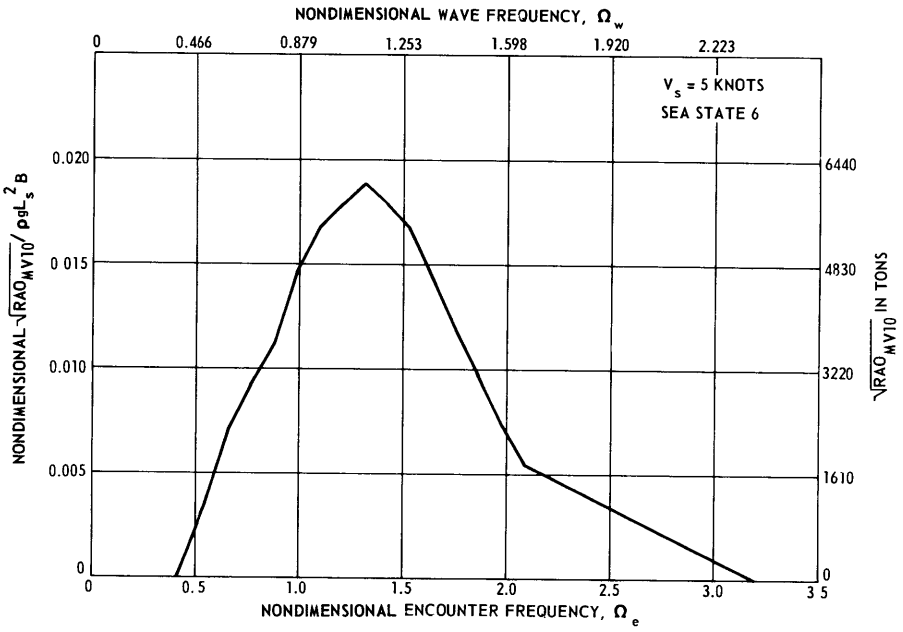

Figure 7 - Root of Midship Vertical Bending Moment RAO, Heading 22.5 Degrees

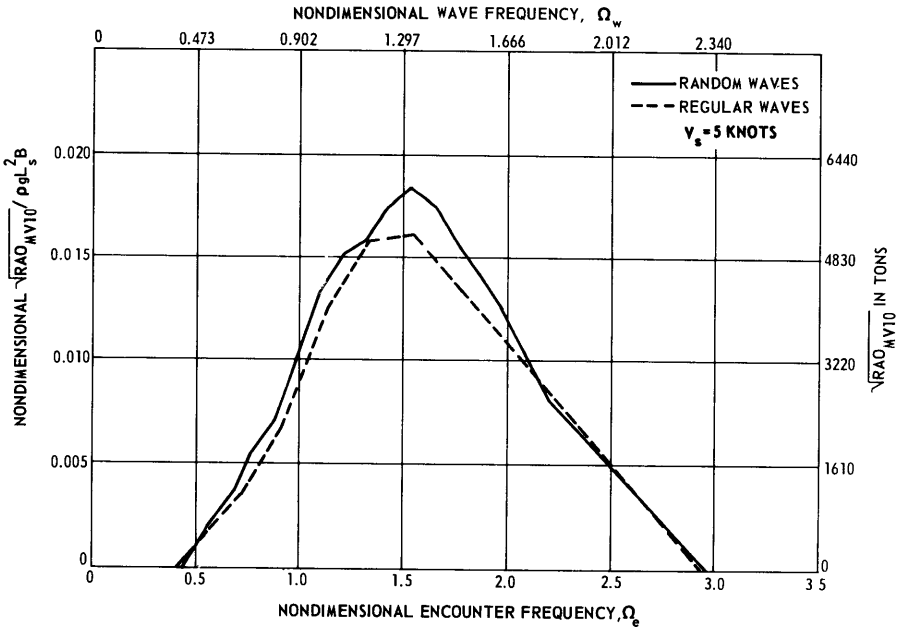

Figure 8 - Root of Midship Vertical Bending Moment RAO, Heading 45 Degrees

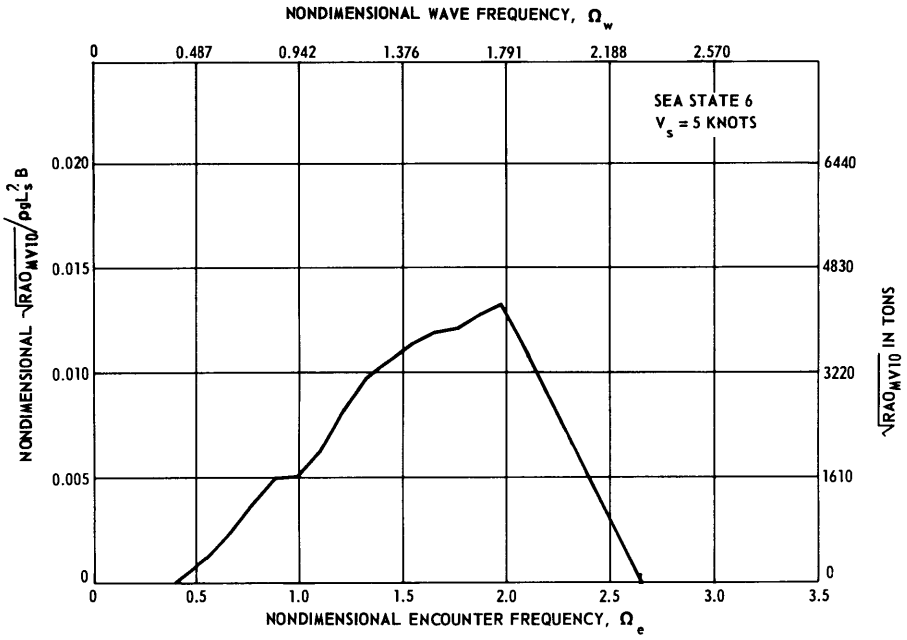

Figure 9 - Root of Midship Vertical Bending Moment RAO, Heading 67.5 Degrees

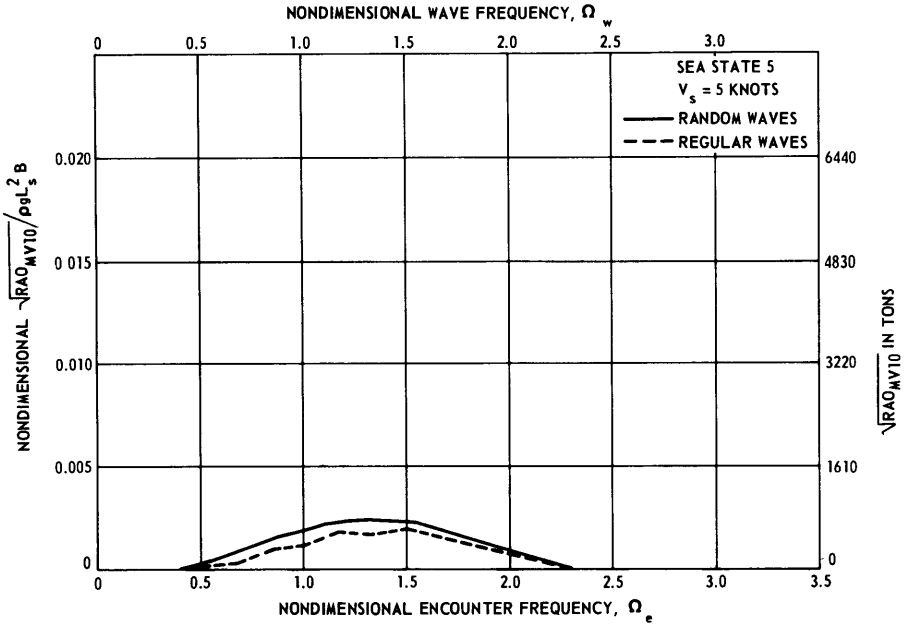

Figure 10 - Root of Midship Vertical Bending Moment RAO, Heading 90 Degrees

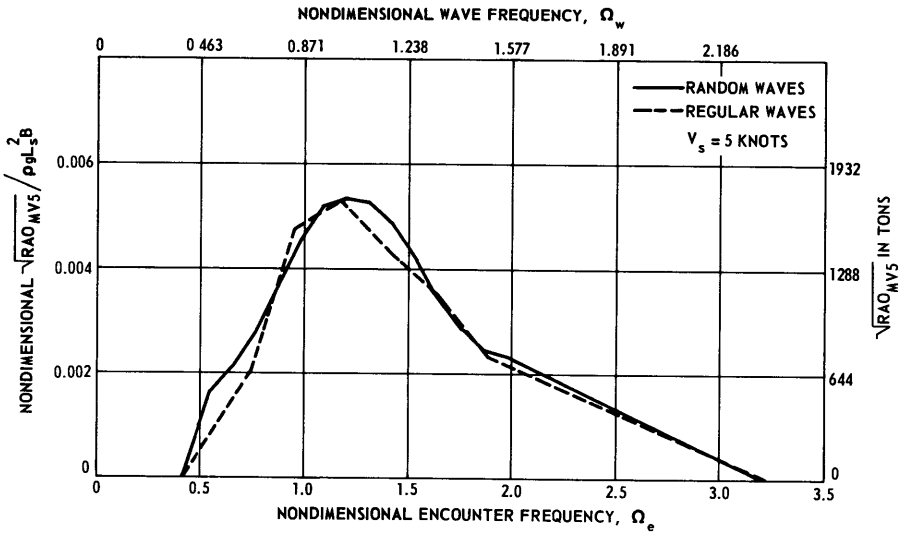

Figure 11 - Root of Station 5 Vertical Bending Moment RAO, Heading Zero

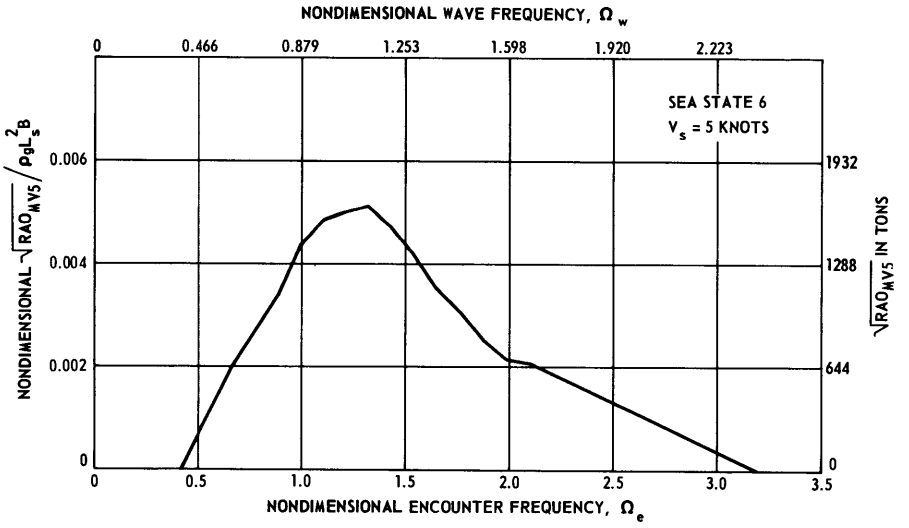

Figure 12 - Root of Station 5 Vertical Bending Moment RAO, Heading 22.5 Degrees

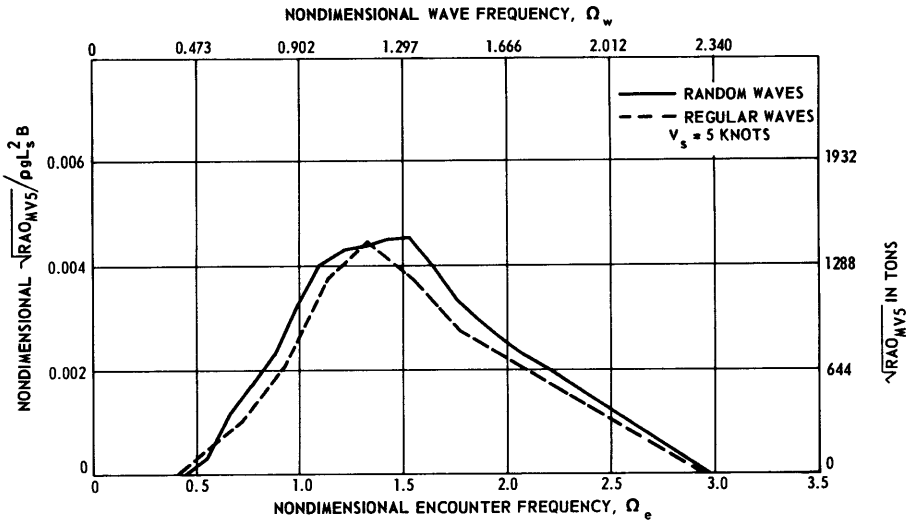

Figure 13 - Root of Station 5 Vertical Bending Moment RAO, Heading 45 Degrees

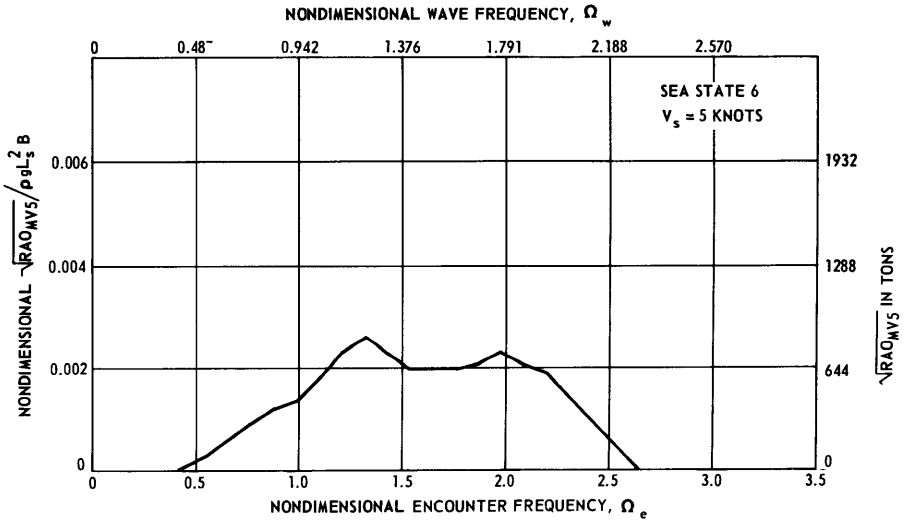

Figure 14 - Root of Station 5 Vertical Bending Moment RAO, Heading 67.5 Degrees

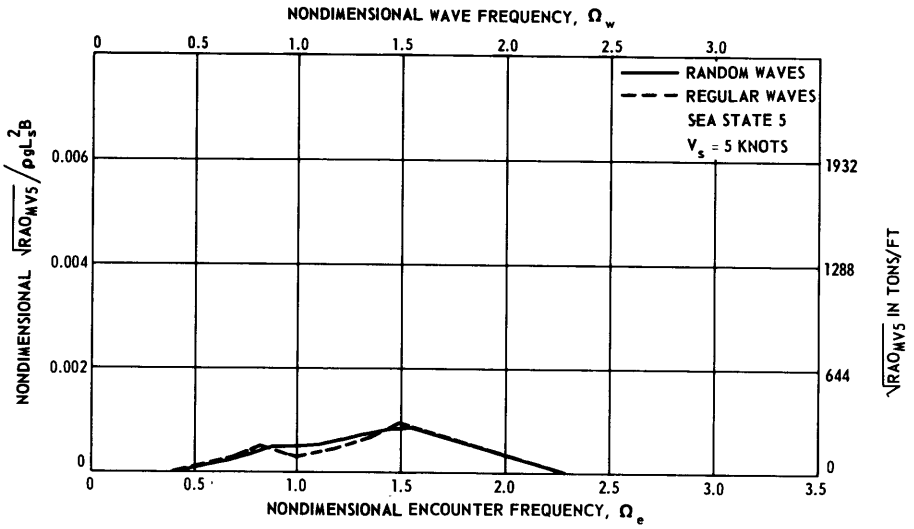

Figure 15 - Root of Station 5 Vertical Bending Moment RAO, Heading 90 Degrees

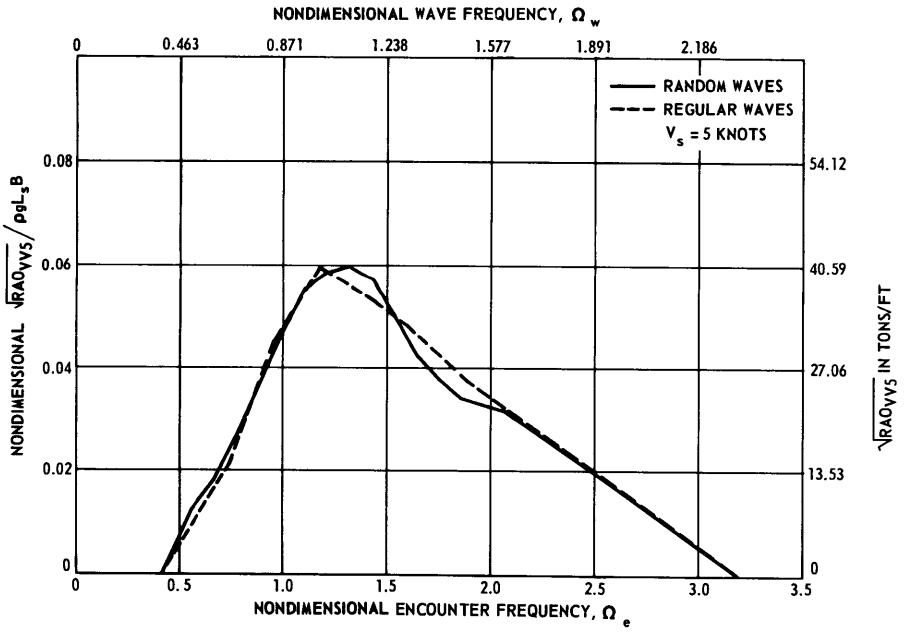

Figure 16 - Root of Station 5 Vertical Shear RAO, Heading Zero

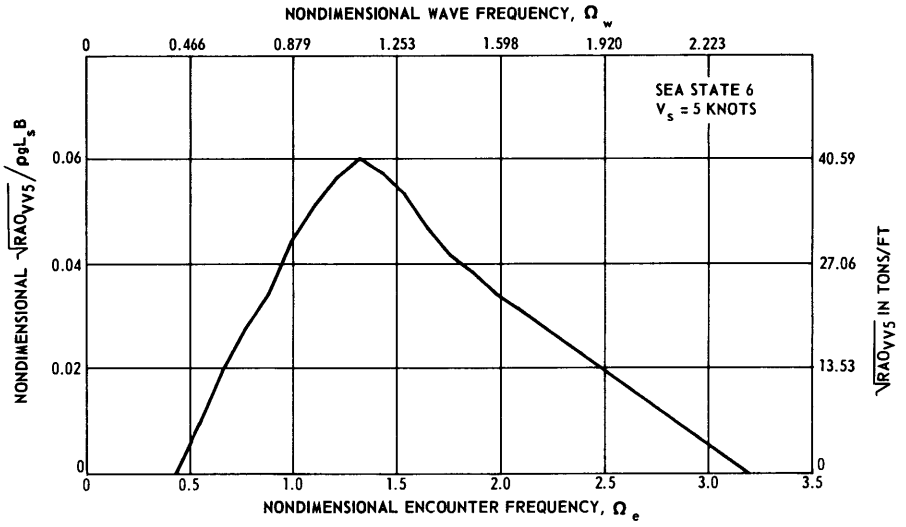

Figure 17 - Root of Station 5 Vertical Shear RAO, Heading 22.5 Degrees

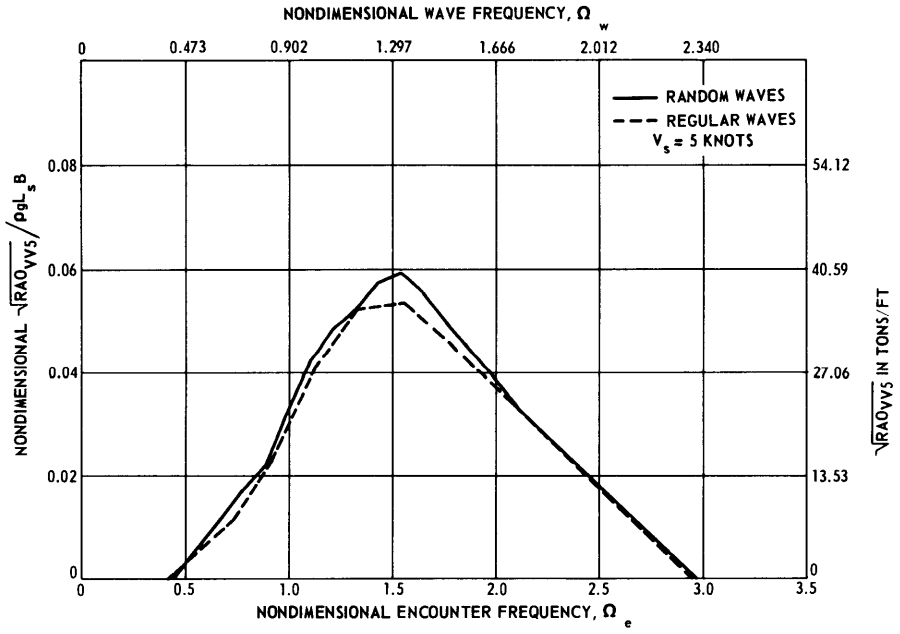

Figure 18 - Root of Station 5 Vertical Shear RAO, Heading 45 Degrees

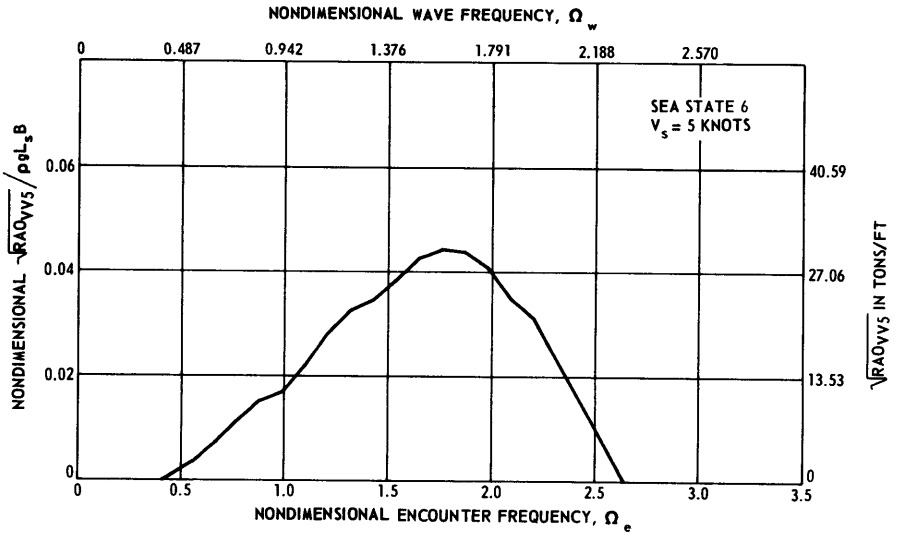

Figure 19 - Root of Station 5 Vertical Shear RAO, Heading 67.5 Degrees

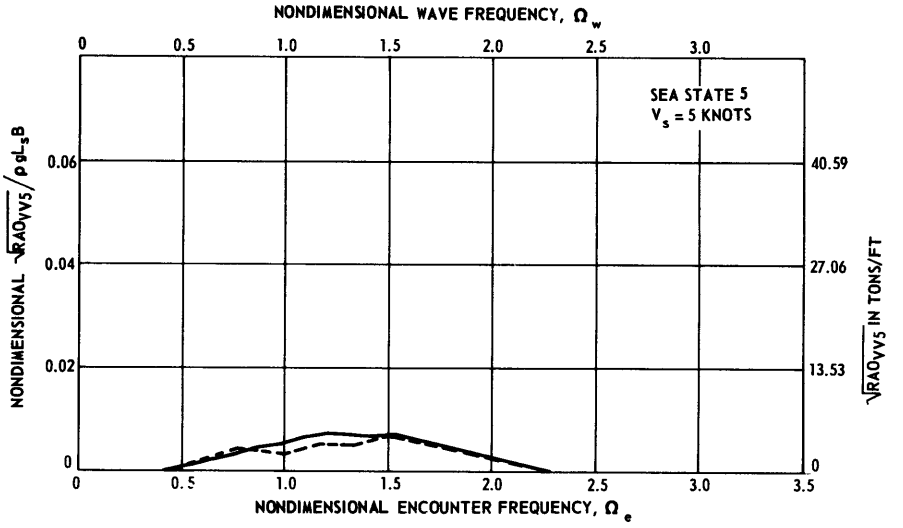

Figure 20 - Root of Station 5 Vertical Shear RAO, Heading 90 Degrees

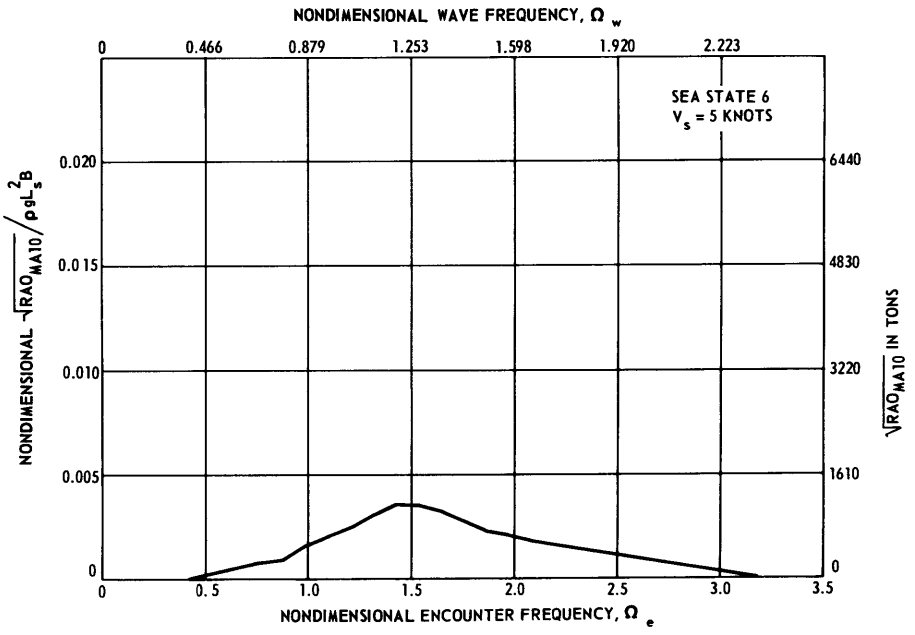

Figure 21 - Root of Midship Transverse Bending Moment RAO, Heading 22.5 Degrees

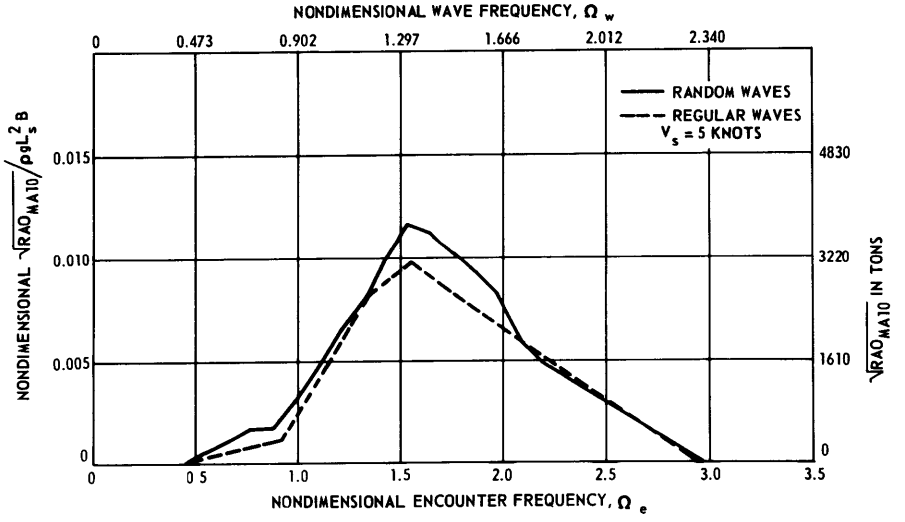

Figure 22 - Root of Midship Transverse Bending Moment RAO, 45 Degrees

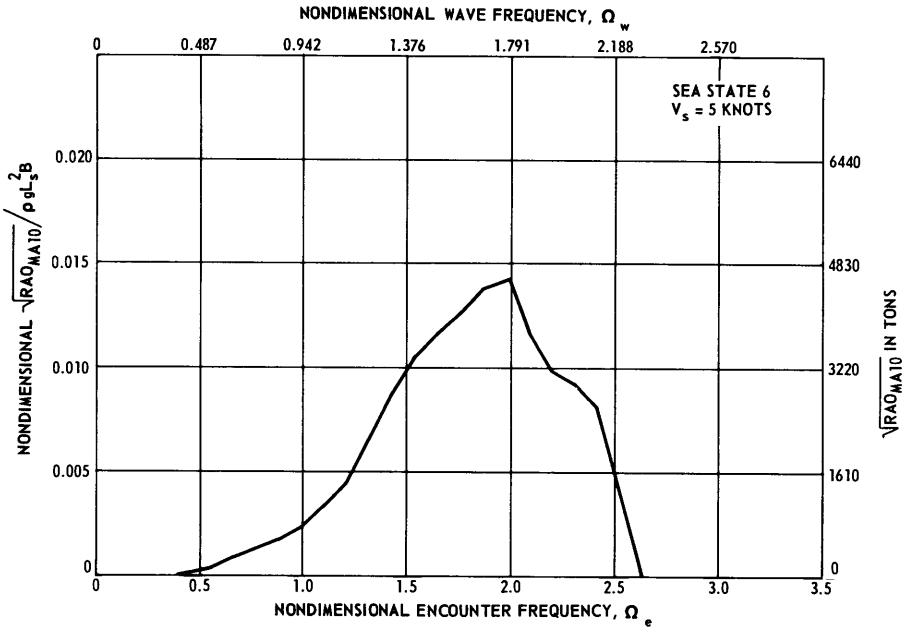

Figure 23 - Root of Midship Transverse Bending Moment RAO, Heading 67.5 Degrees

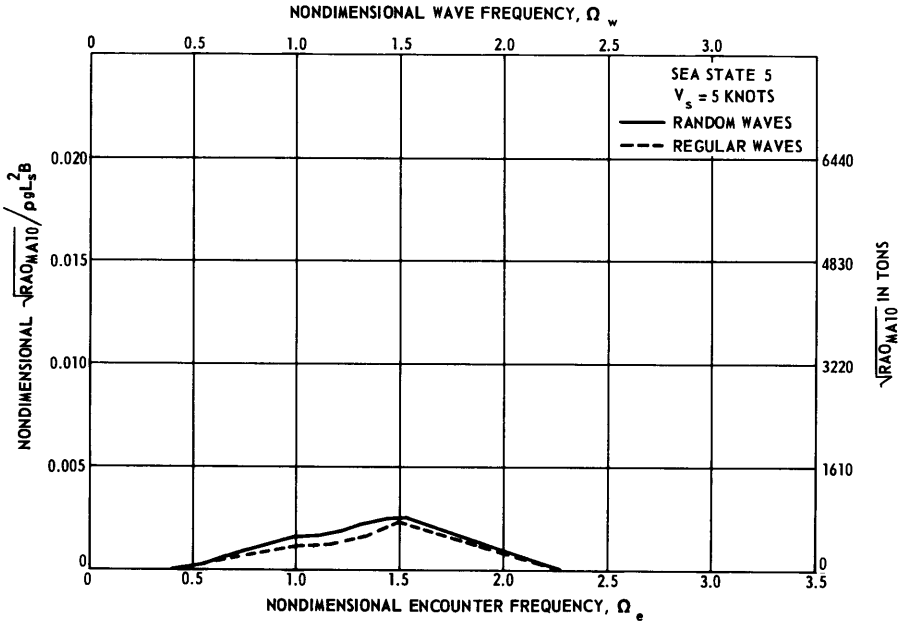

Figure 24 - Root of Midship Transverse Bending Moment RAO, Heading 90 Degrees

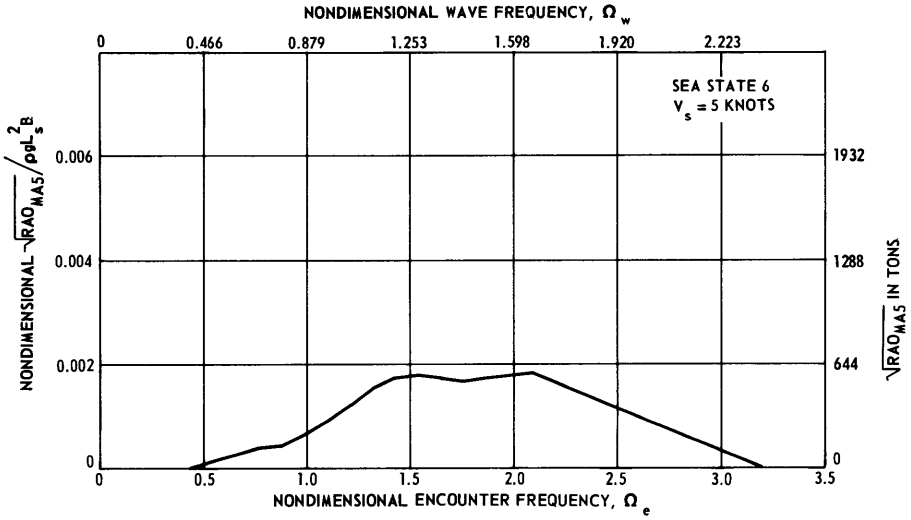

Figure 25 - Root of Station 5 Transverse Bending Moment RAO, Heading 22.5 Degrees

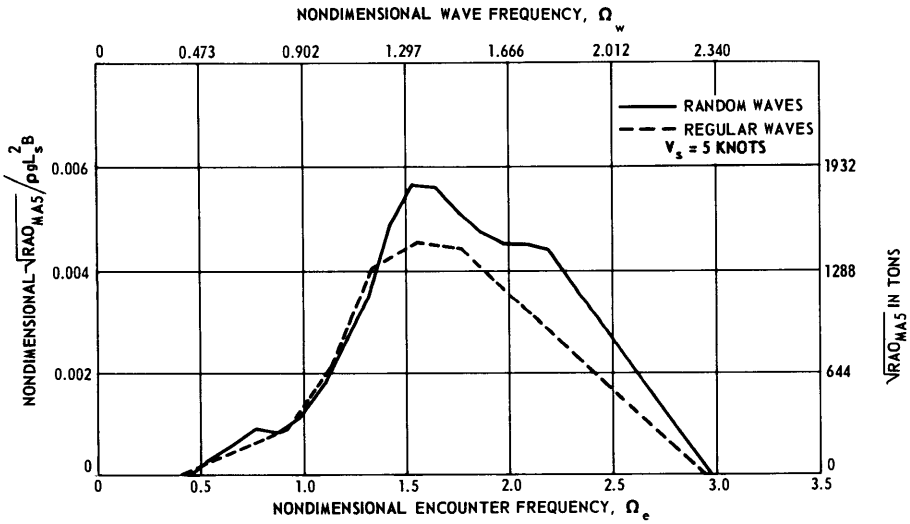

Figure 26 - Root of Station 5 Transverse Bending Moment RAO, Heading 45 Degrees

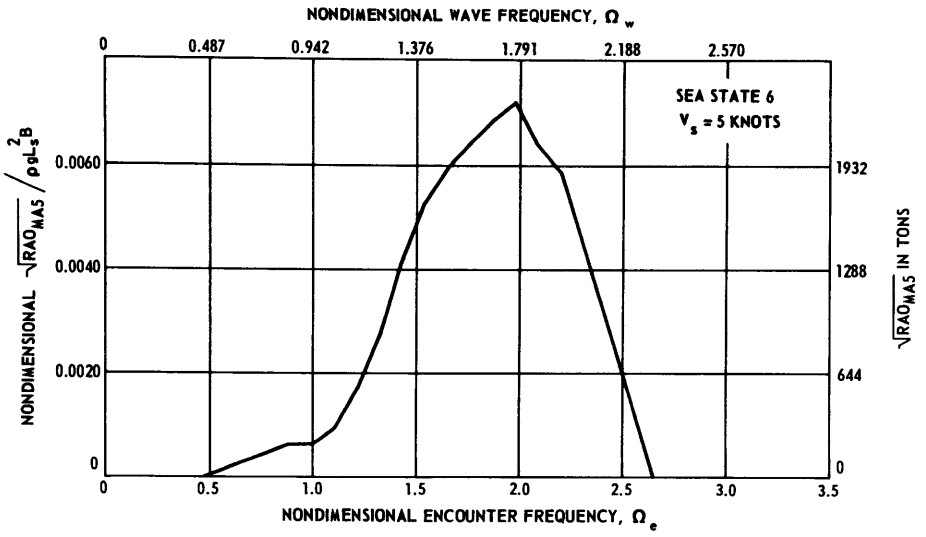

Figure 27 - Root of Station 5 Transverse Bending Moment RAO, Heading 67.5 Degrees

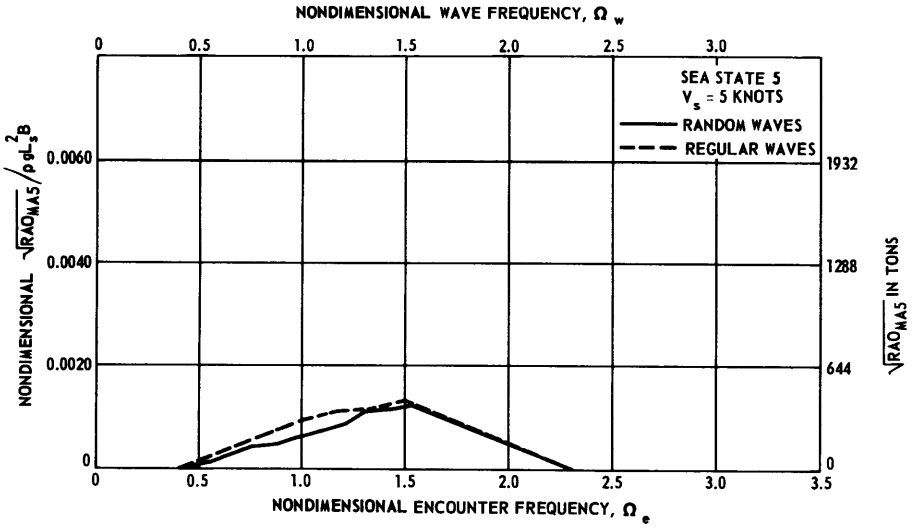

Figure 28 - Root of Station 5 Transverse Bending Moment RAO, Heading 90 Degrees

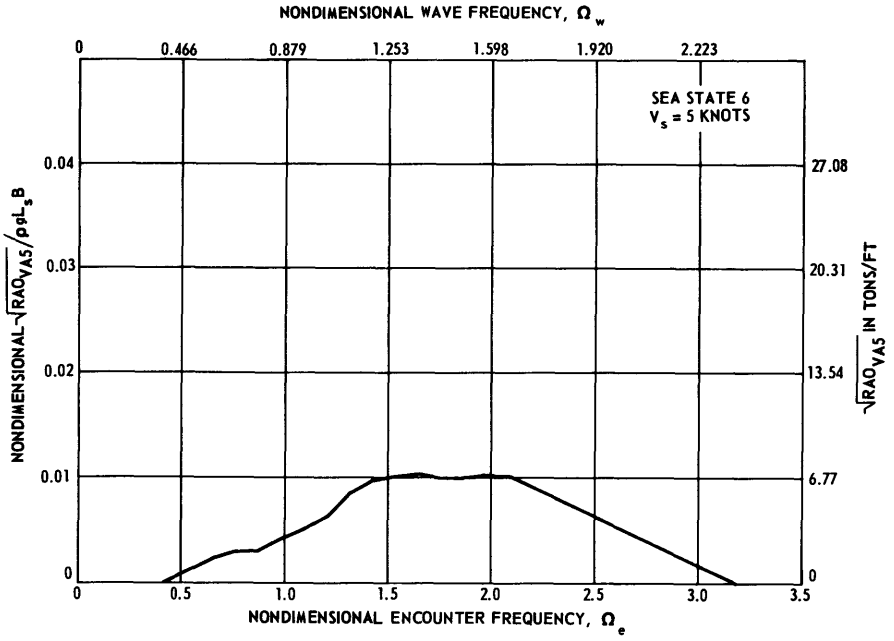

Figure 29 - Root of Station 5 Transverse Shear RAO, Heading 22.5 Degrees

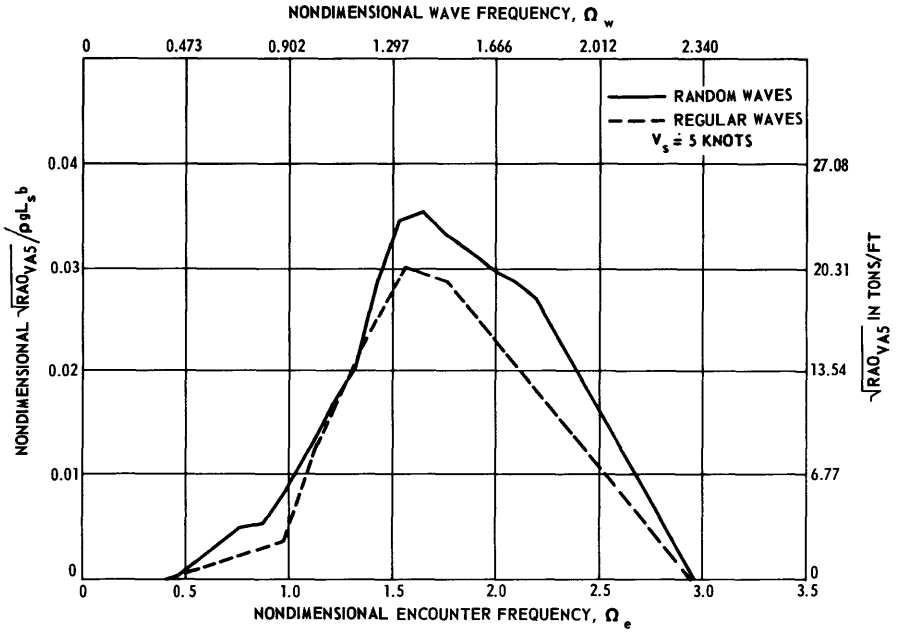

Figure 30 - Root of Station 5 Transverse Shear RAO, Heading 45 Degrees

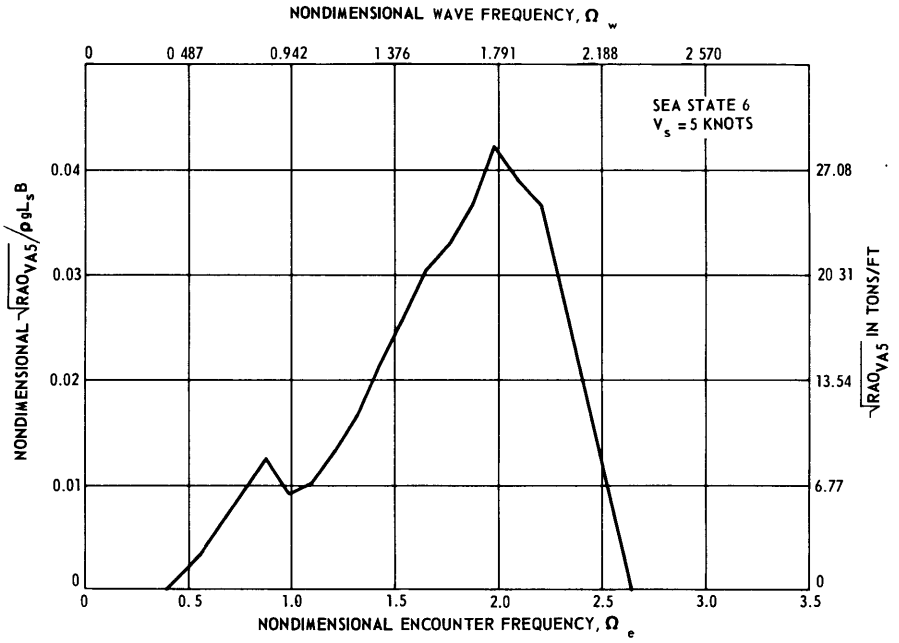

Figure 31 - Root of Station 5 Transverse Shear RAO, Heading 67.5 Degrees

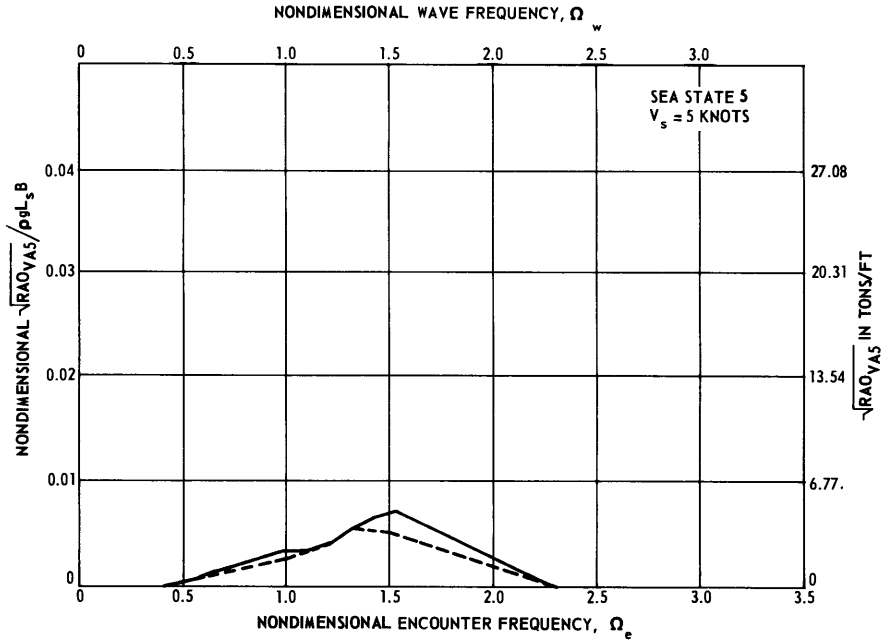

Figure 32 - Root of Station 5 Transverse Shear RAO, Heading 90 Degrees

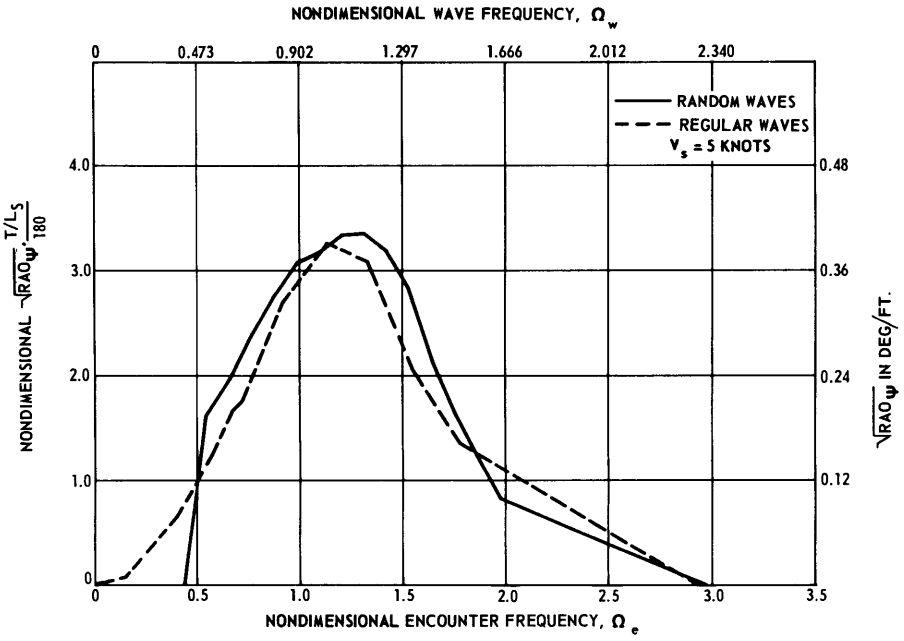

Figure 33 - Root of Pitch Angle RAO, Heading 45 Degrees

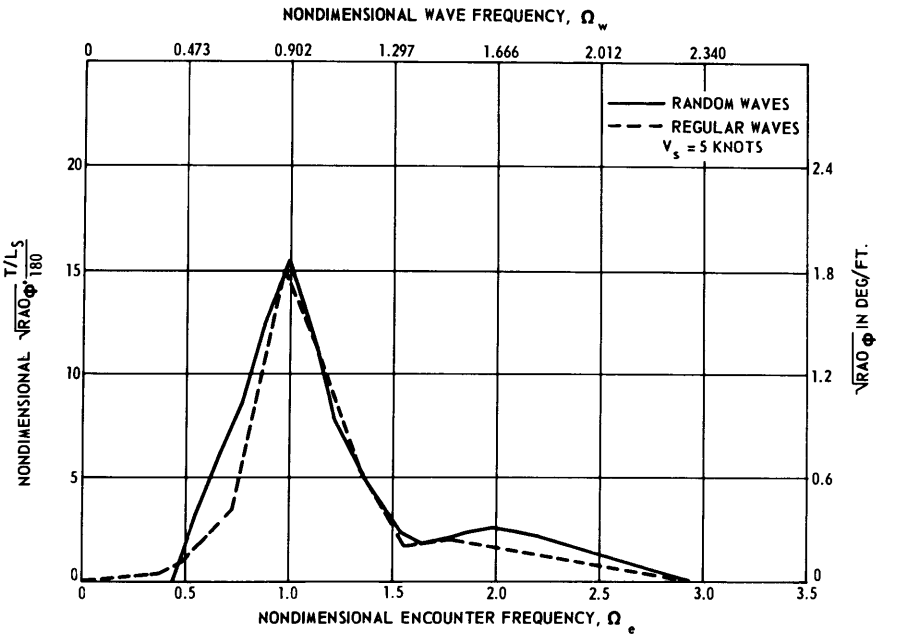

Figure 34 - Root of Roll Angle RAO, Heading 45 Degrees

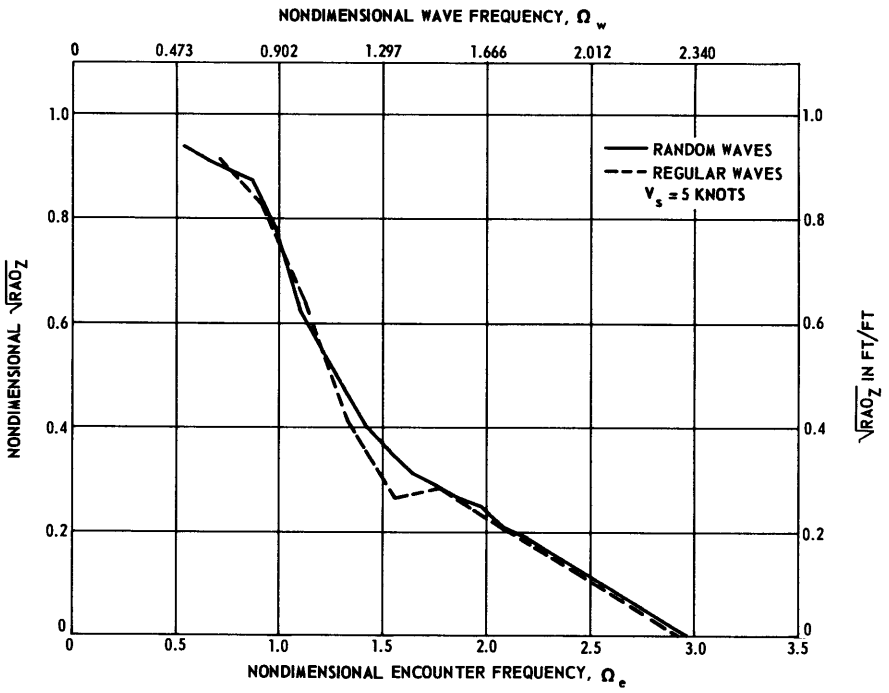

Figure 35 - Root of Heave Displacement RAO, Heading 45 Degrees

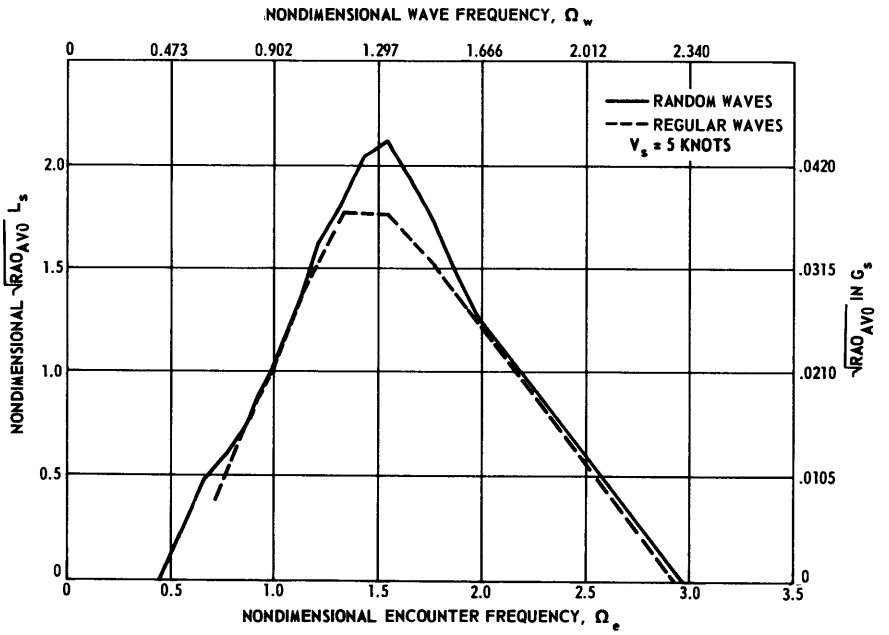

Figure 36 - Root of Bow Acceleration RAO, Heading 45 Degrees

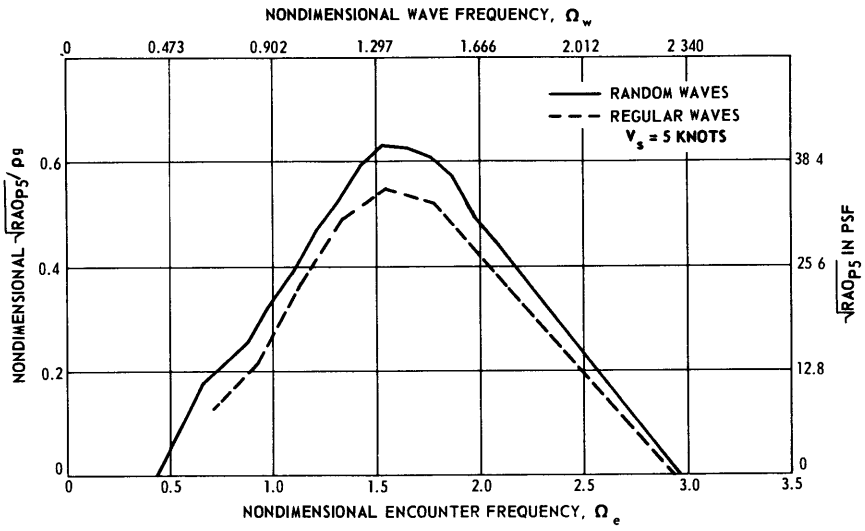

Figure 37 - Root of Bow Pressure RAO, Heading 45 Degrees

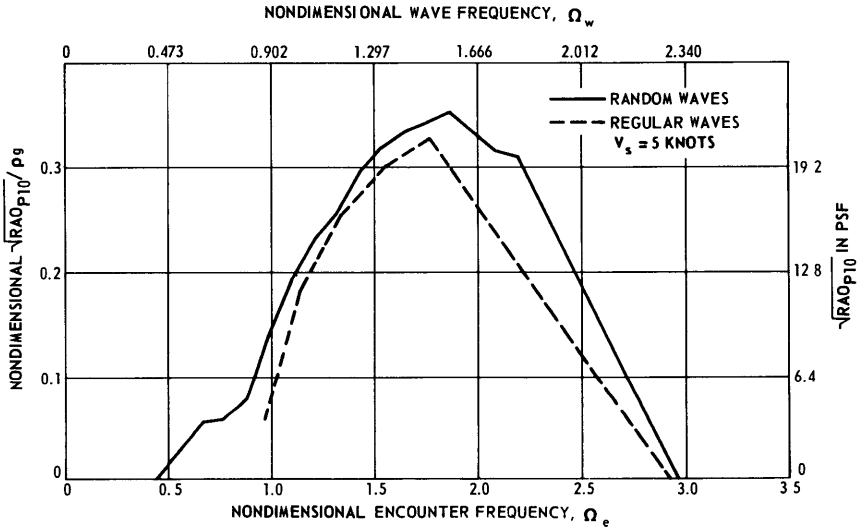

Figure 38 - Root of Midship Pressure RAO, Heading 45 Degrees

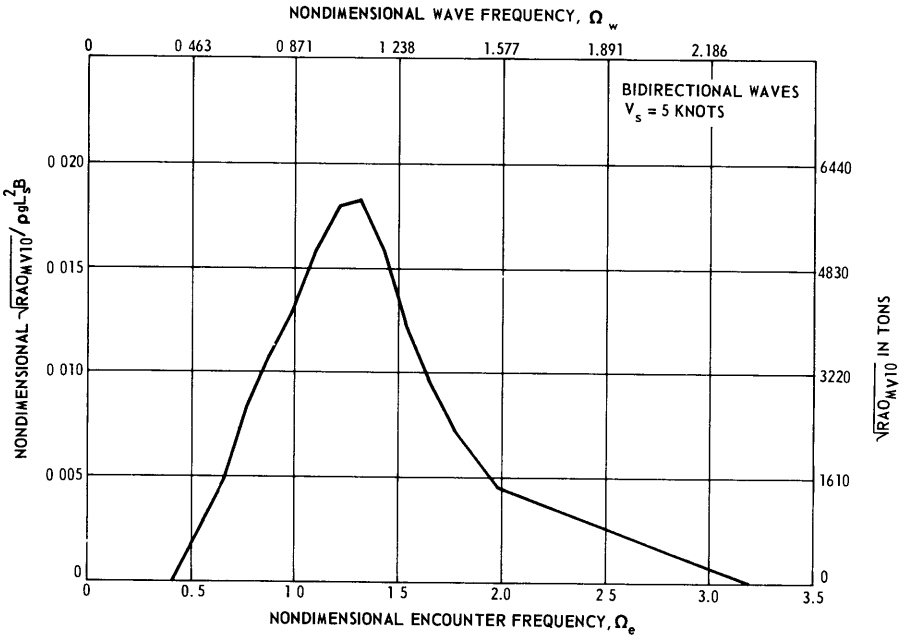

Figure 39 - Root of Midship Vertical Bending Moment RAO, Heading Zero

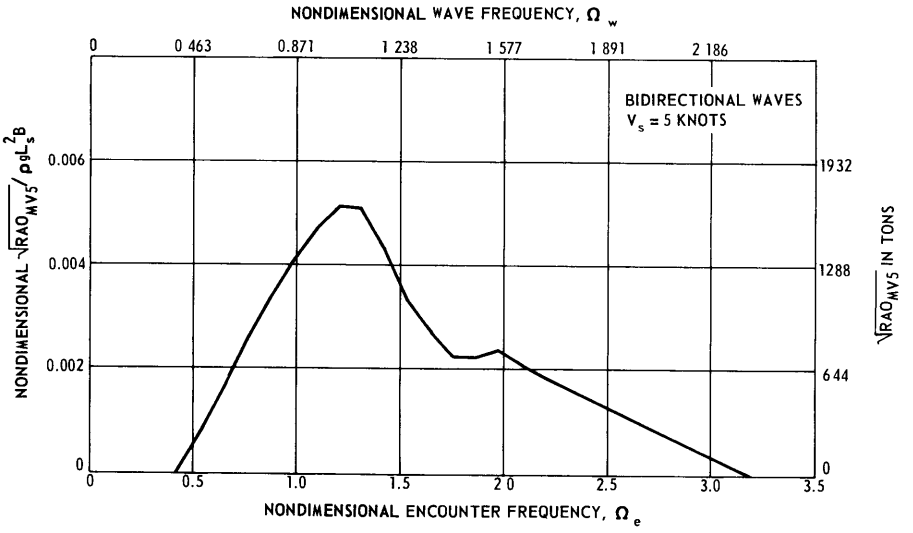

Figure 40 - Root of Station 5 Vertical Bending Moment RAO, Heading Zero

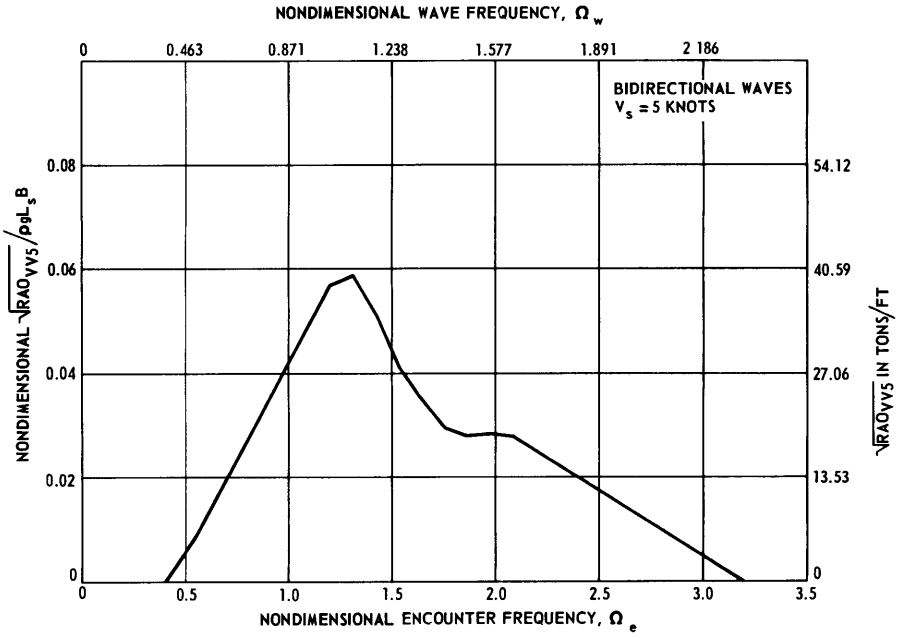

Figure 41 - Root of Station 5 Vertical Shear RAO, Heading Zero

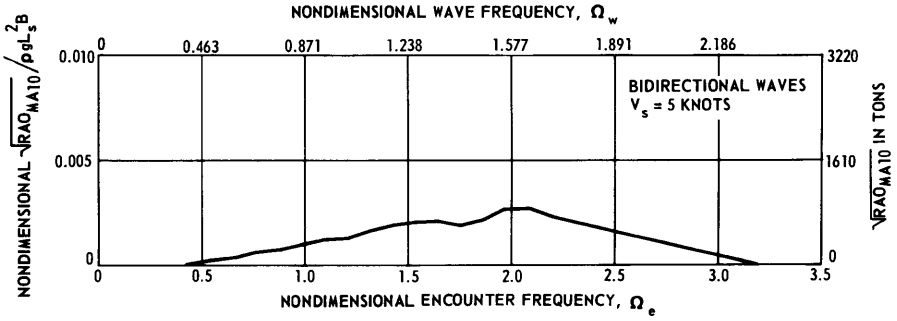

Figure 42 - Root of Midship Transverse Bending Moment RAO, Heading Zero

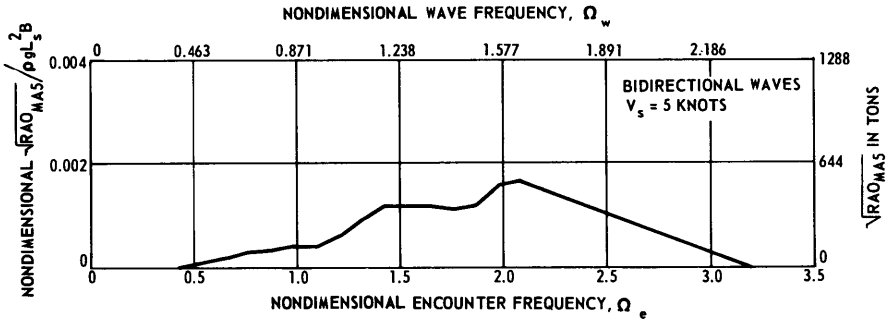

Figure 43 - Root of Station 5 Transverse Bending Moment RAO, Heading Zero

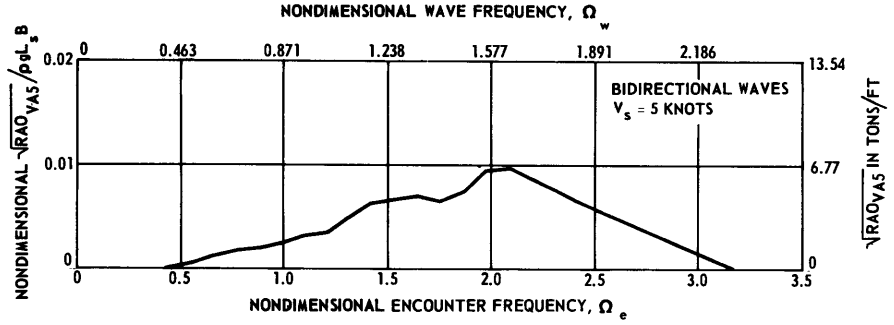

Figure 44 - Root of Station 5 Transverse Shear RAO, Heading Zero

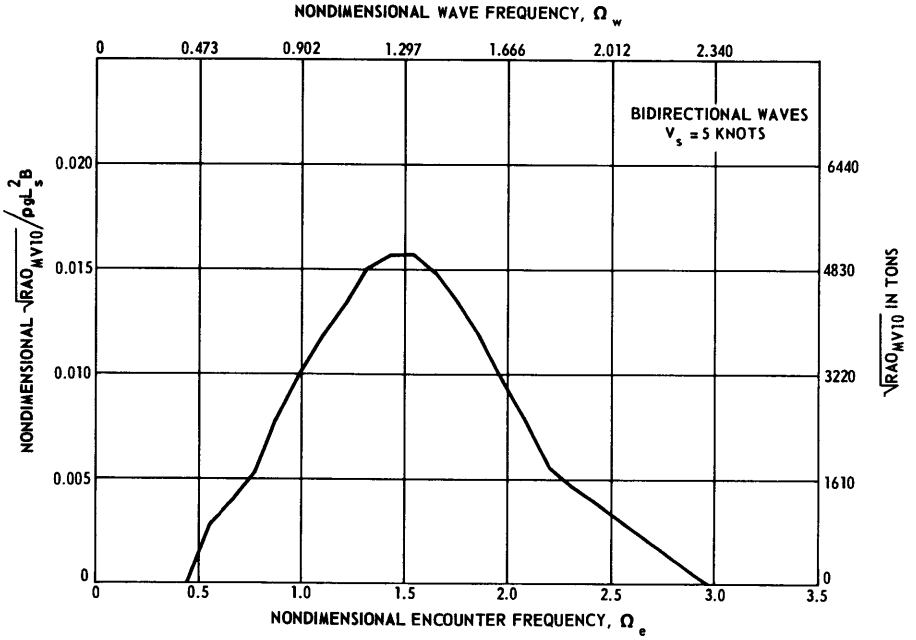

Figure 45 - Root of Midship Vertical Bending Moment RAO, Heading 45 Degrees

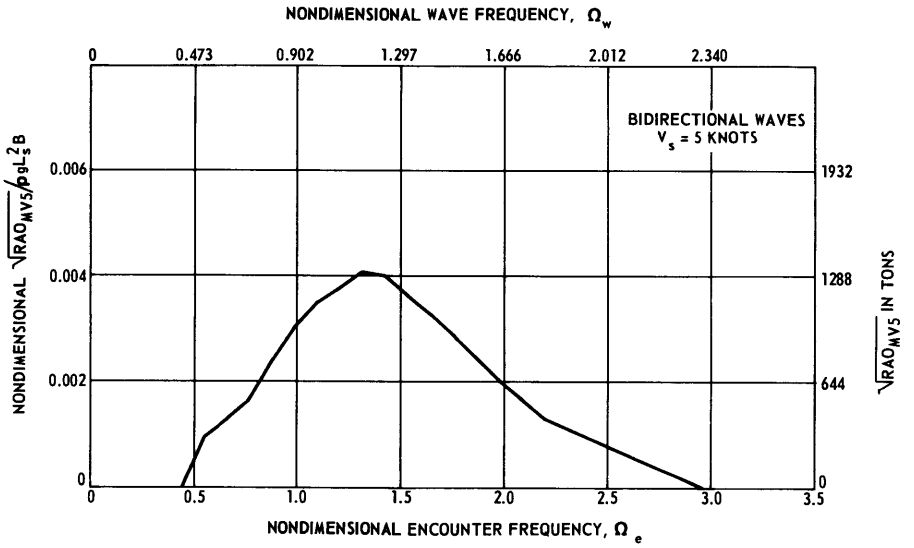

Figure 46 - Root of Station 5 Vertical Bending Moment RAO, Heading 45 Degrees

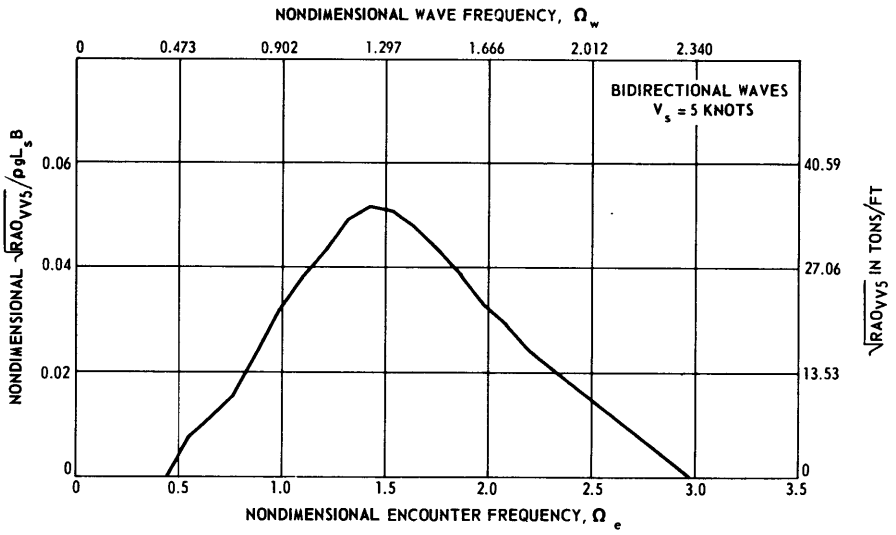

Figure 47 - Root of Station 5 Vertical Shear RAO, Heading 45 Degrees

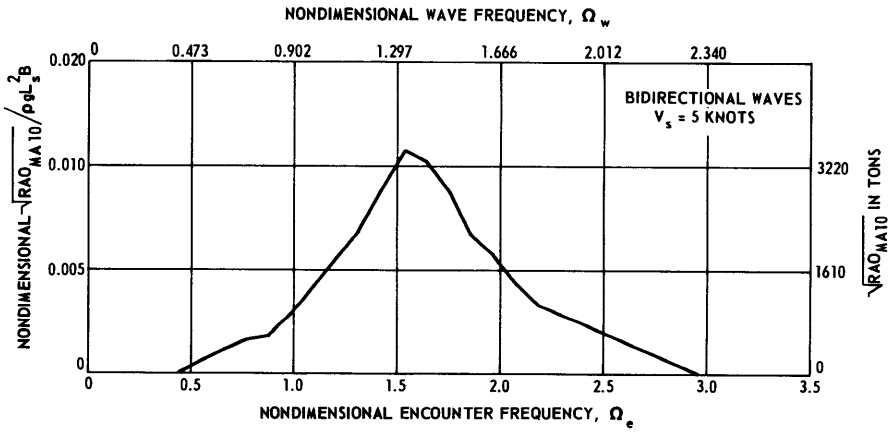

Figure 48 - Root of Midship Transverse Bending Moment RAO, Heading 45 Degrees

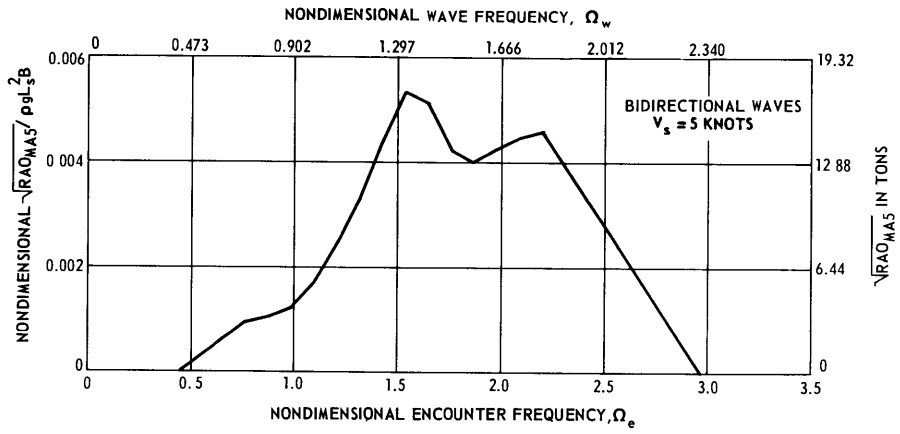

Figure 49 - Root of Station 5 Transverse Bending Moment RAO, Heading 45 Degrees

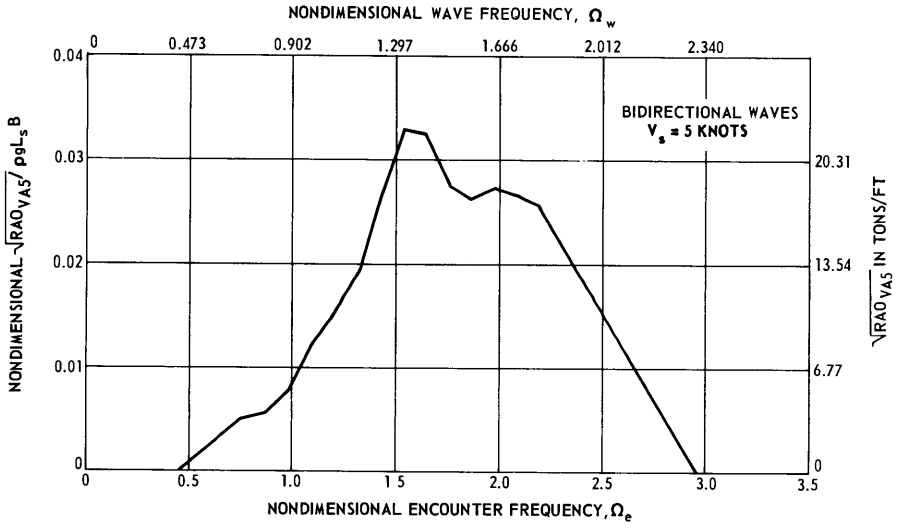

Figure 50 - Root of Station 5 Transverse Shear RAO, Heading 45 Degrees

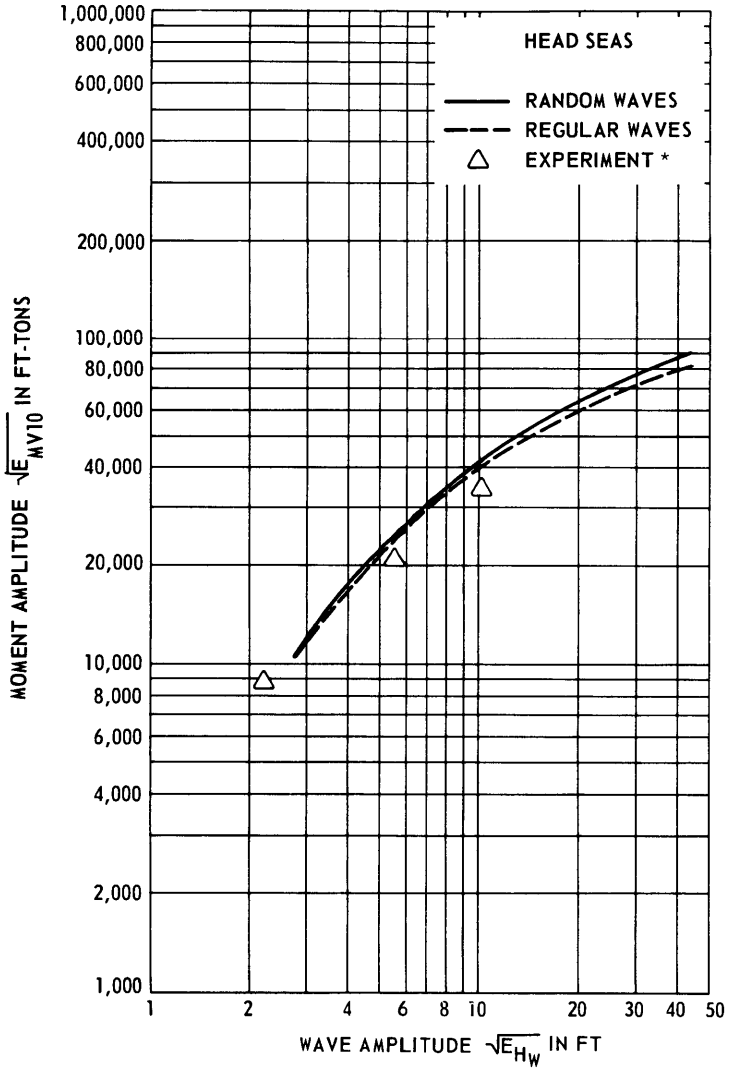

*$\sqrt{E}$ values obtained from tank spectra.

Figure 51 - Midship Vertical Moment Prediction

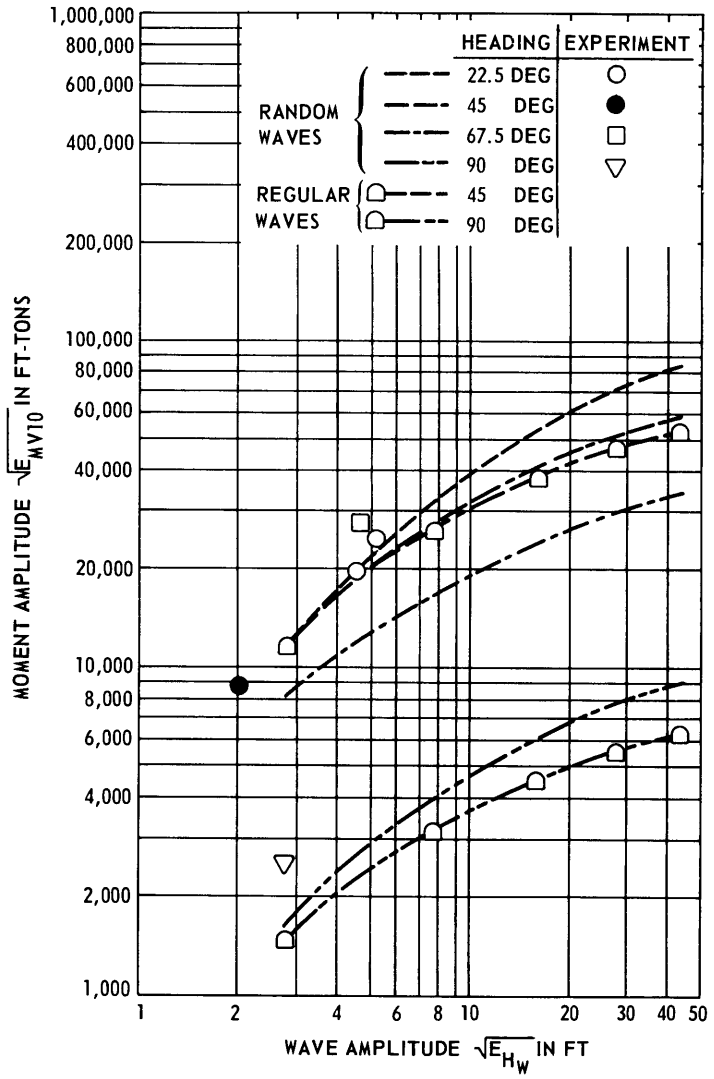

Figure 52 - Midship Vertical Moment Prediction

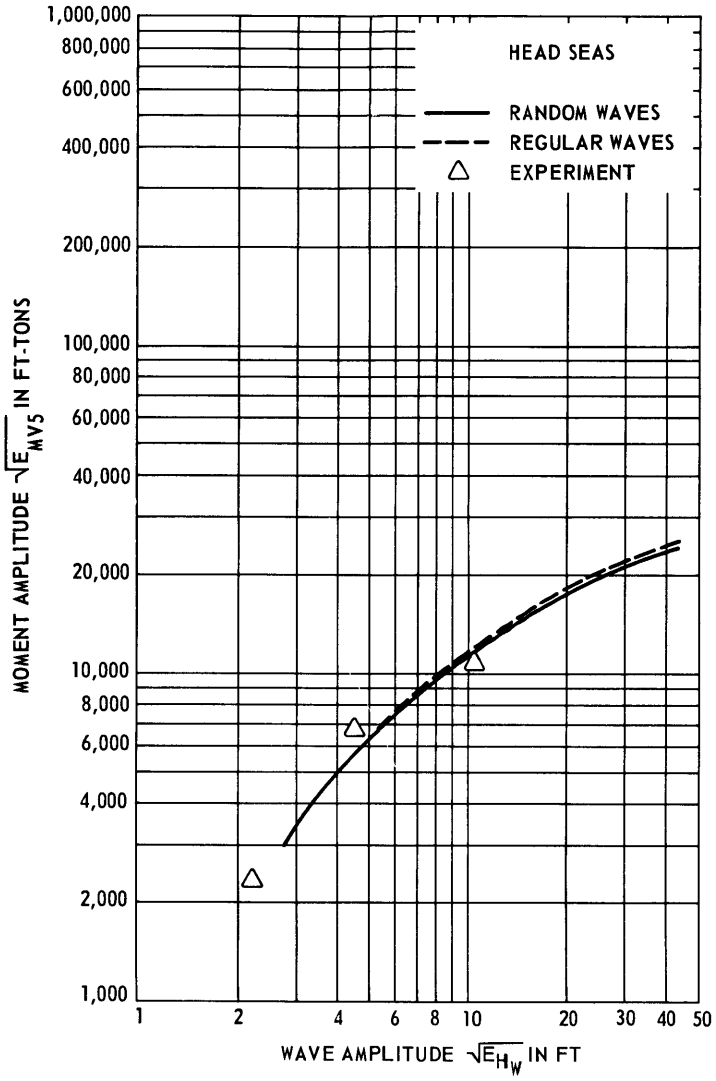

Figure 53 - Station 5 Vertical Moment Prediction

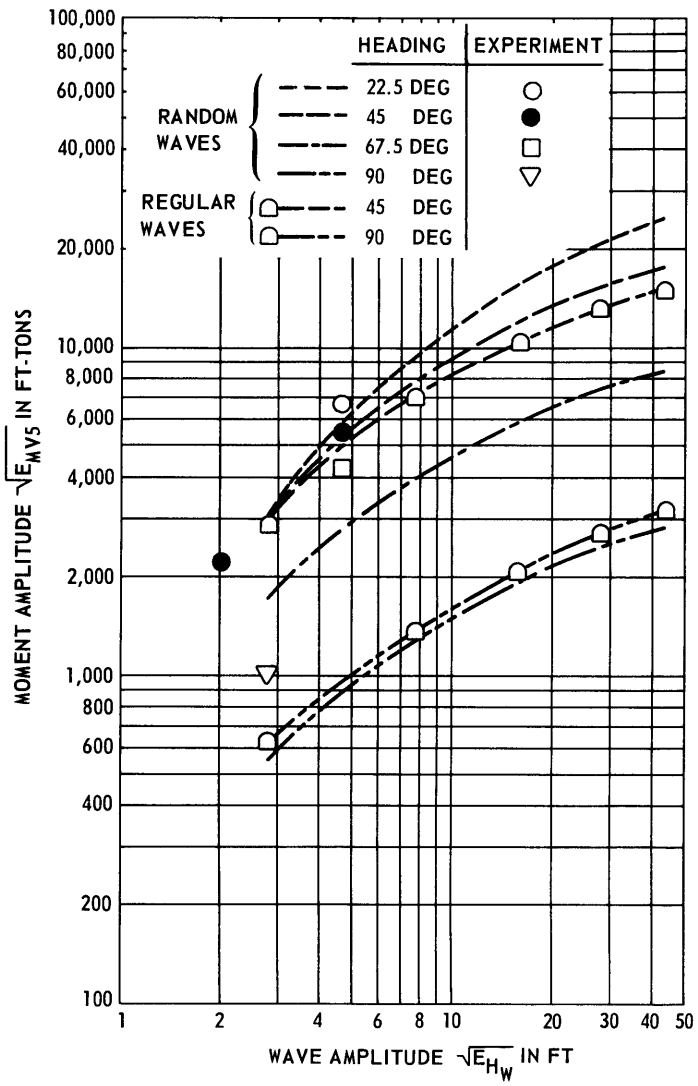

Figure 54 - Station 5 Vertical Moment Prediction

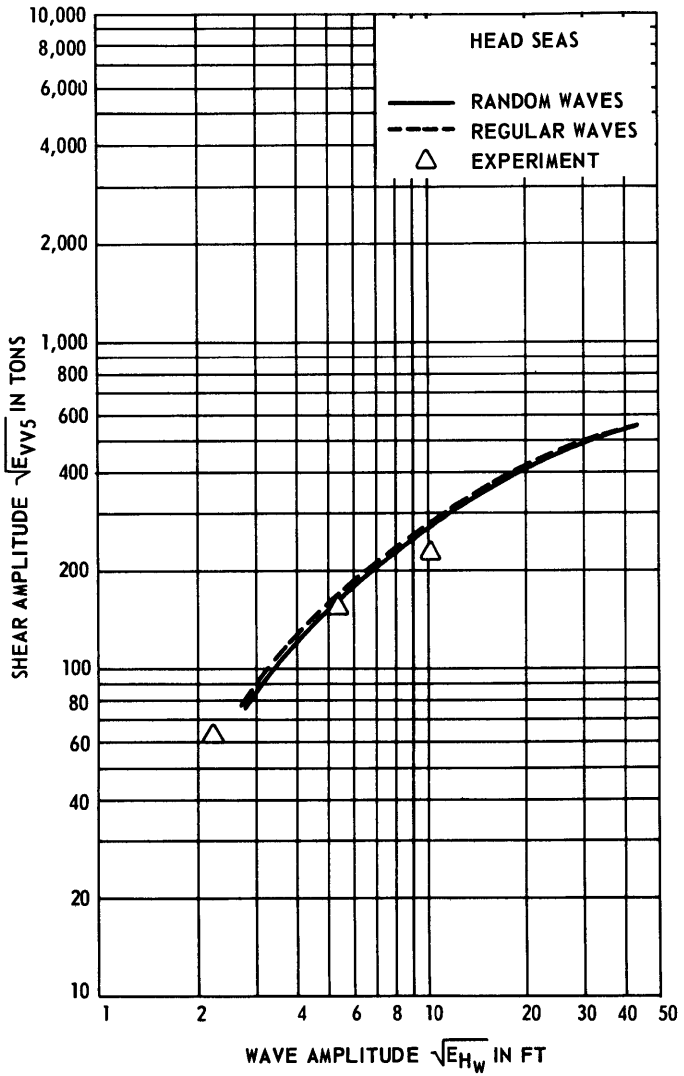

Figure 55 - Station 5 Vertical Shear Prediction

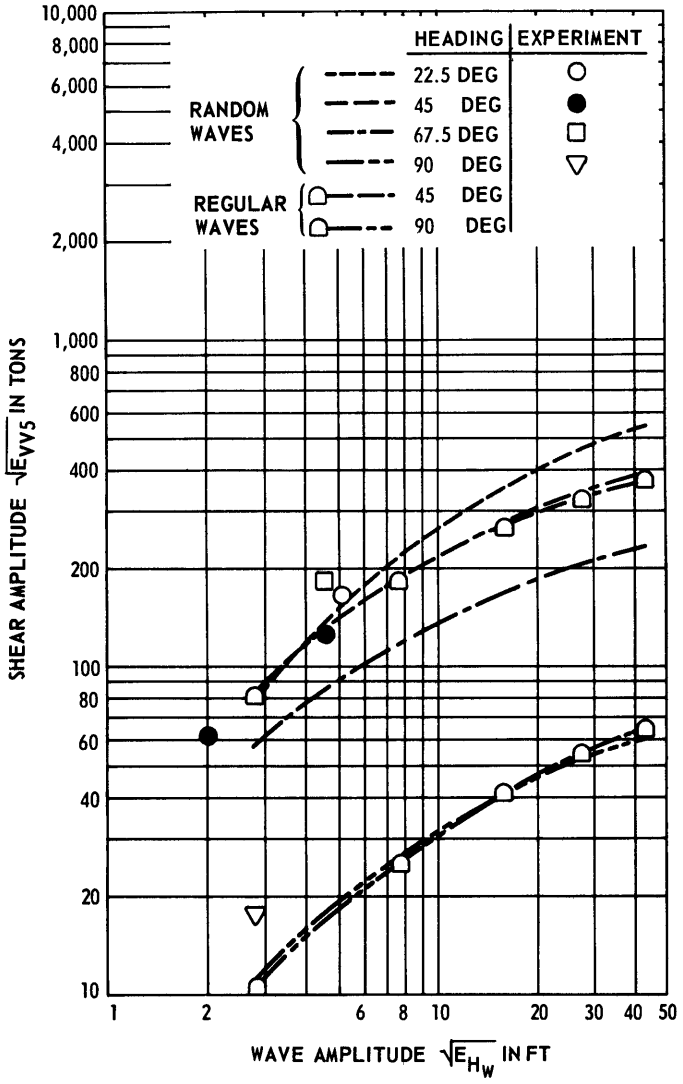

Figure 56 - Station 5 Vertical Shear Prediction

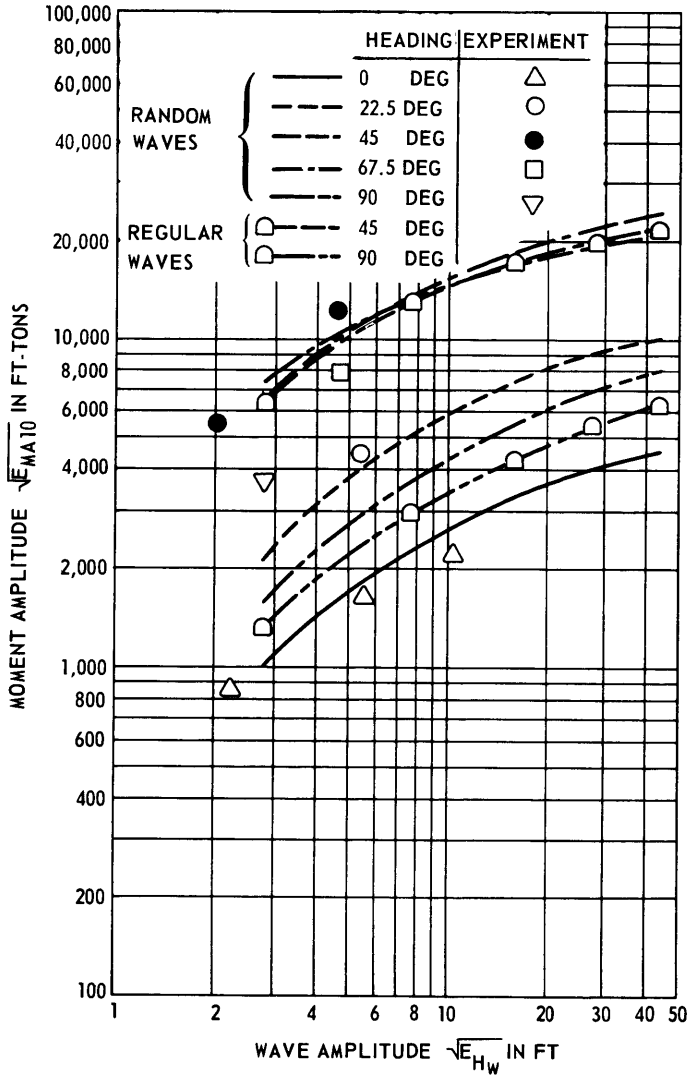

Figure 57 - Midship Transverse Moment Prediction

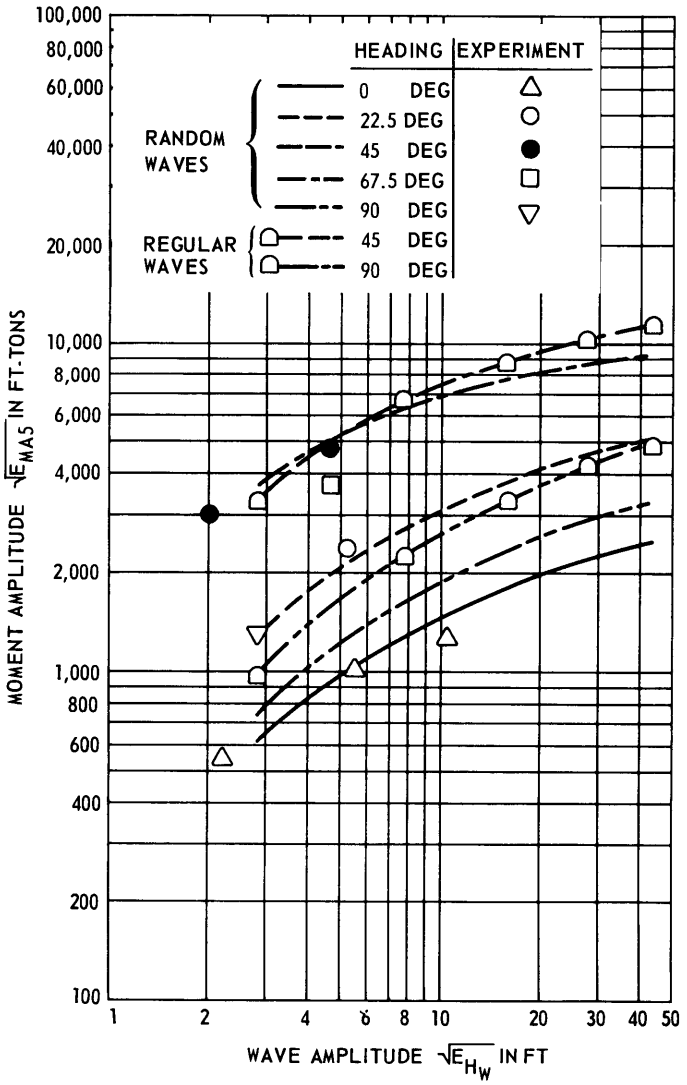

Figure 58 - Station 5 Transverse Moment Prediction

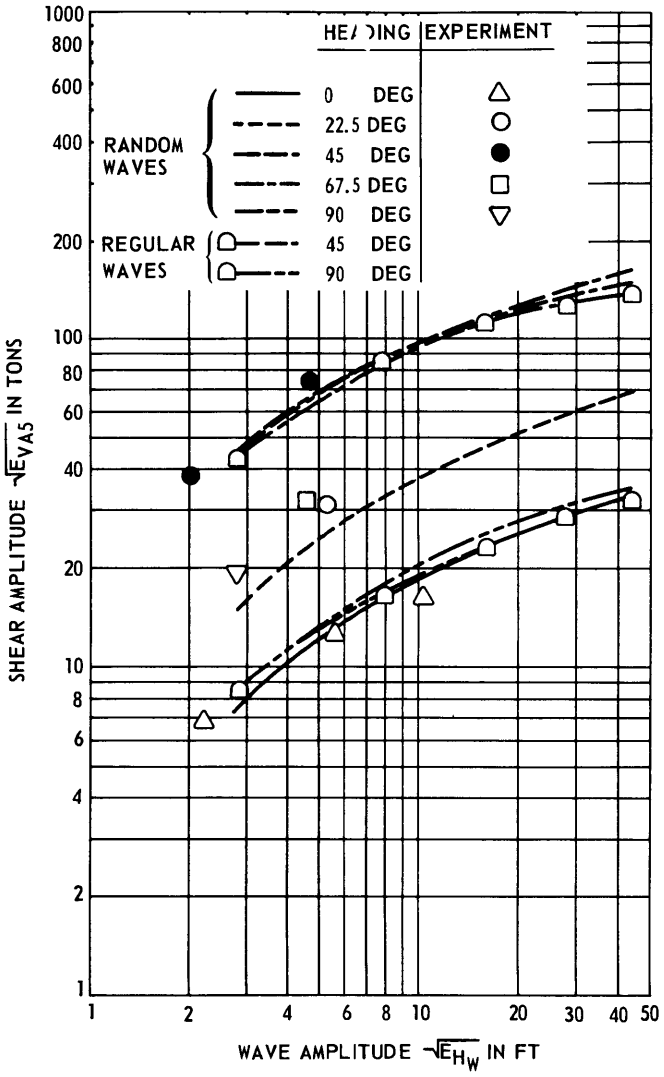

Figure 59 - Station 5 Transverse Shear Prediction

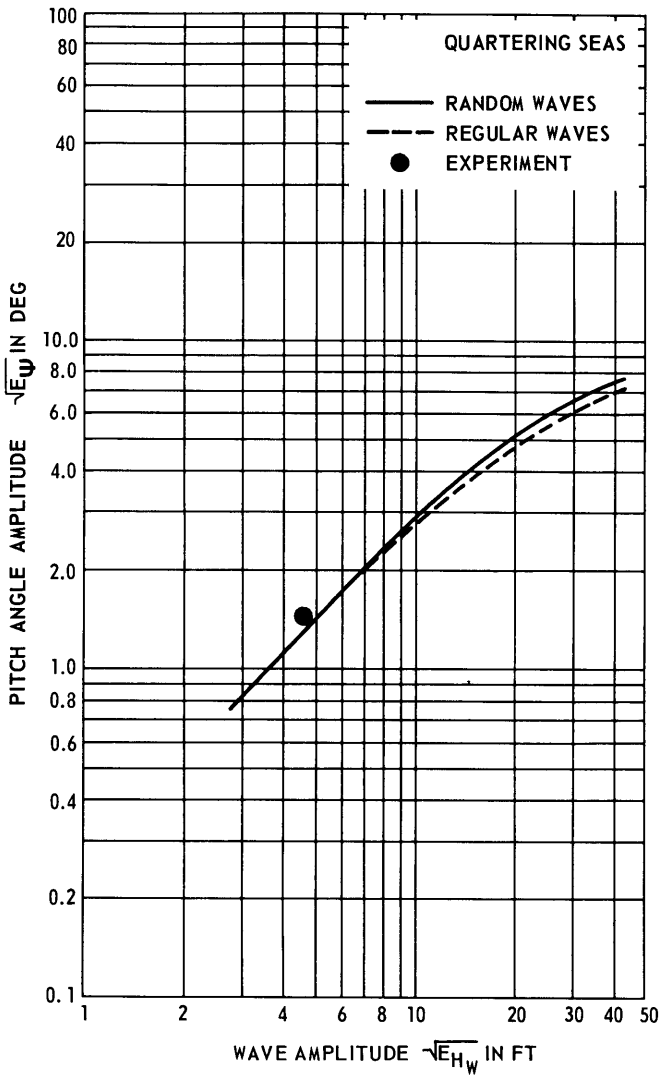

Figure 60 - Pitch Angle Prediction

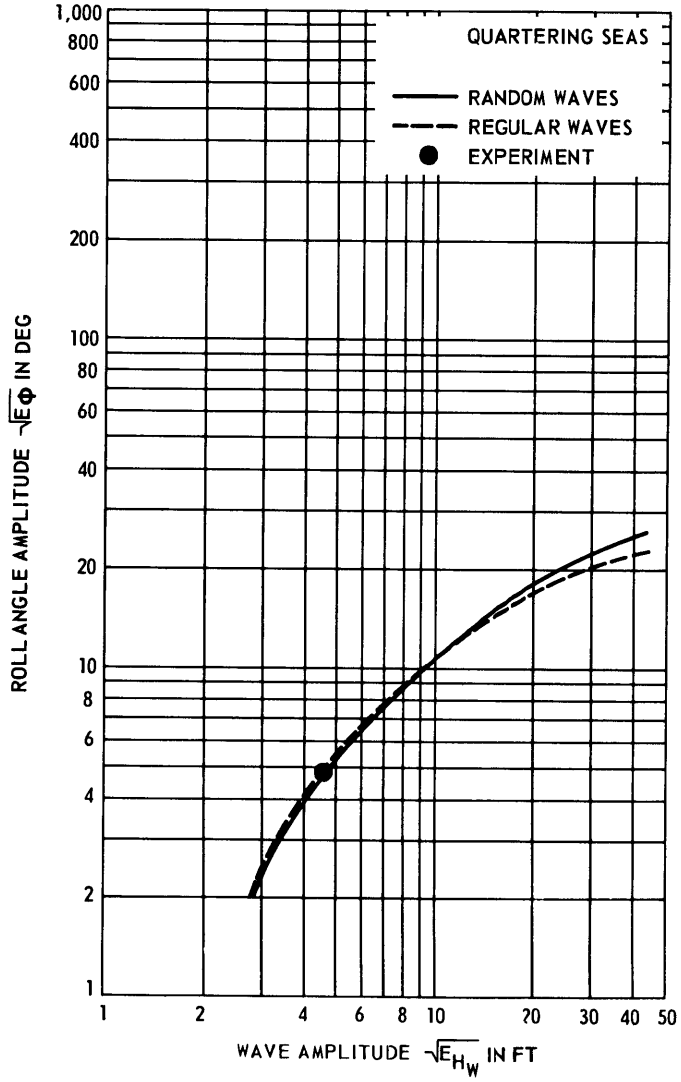

Figure 61 - Roll Angle Prediction

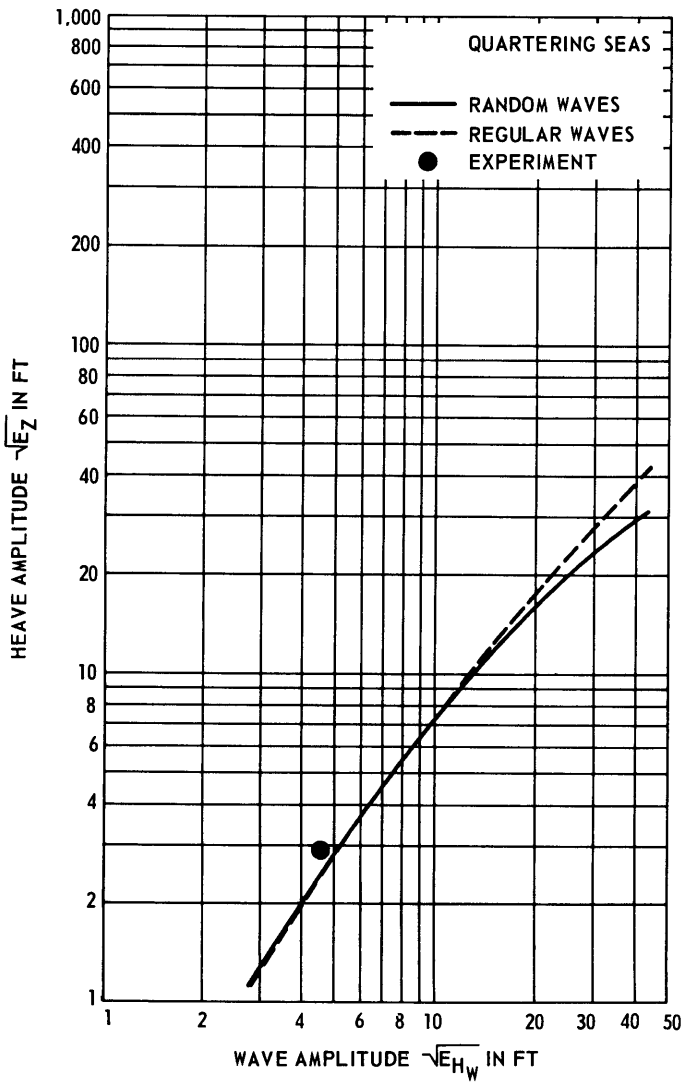

Figure 62 - Heave Displacement Prediction

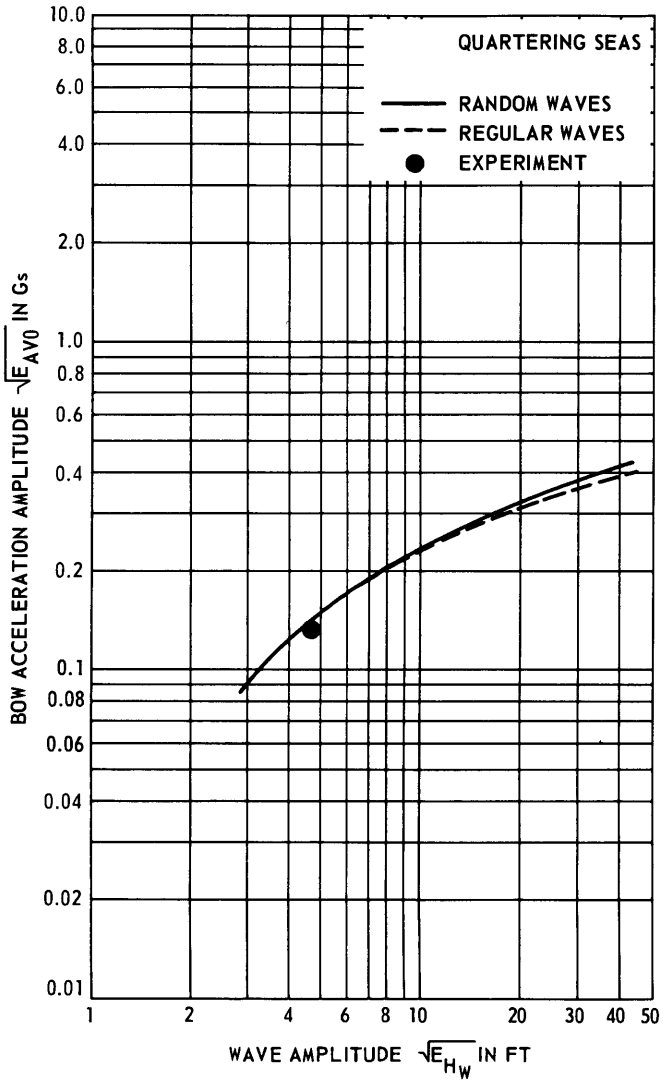

Figure 63 - Bow Acceleration Prediction

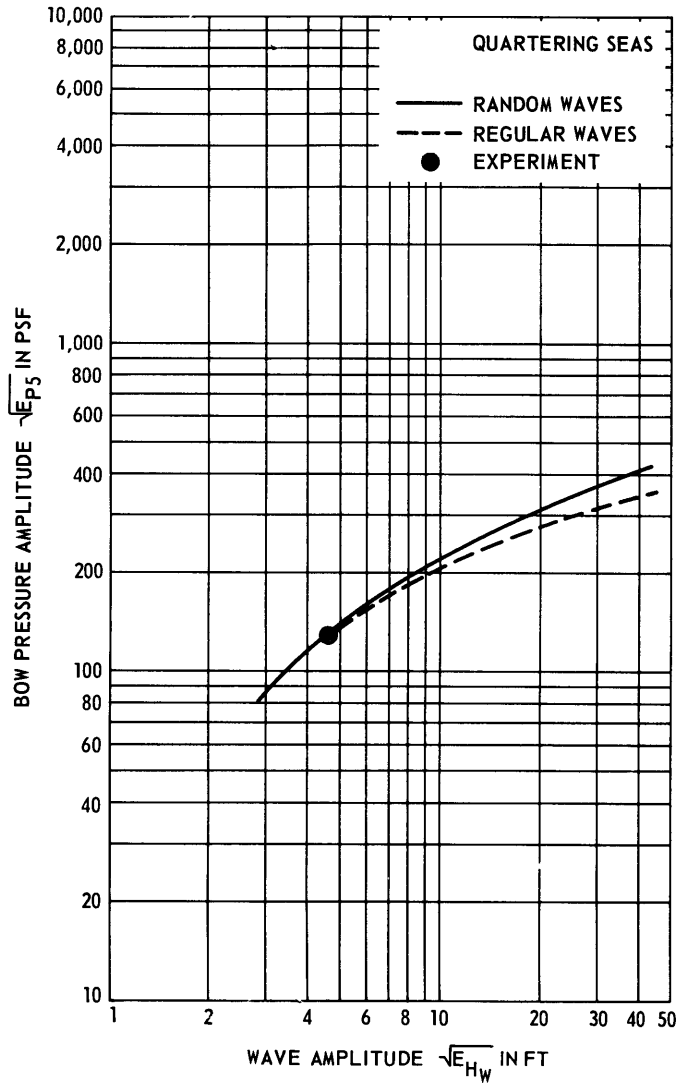

Figure 64 - Bow Pressure Prediction

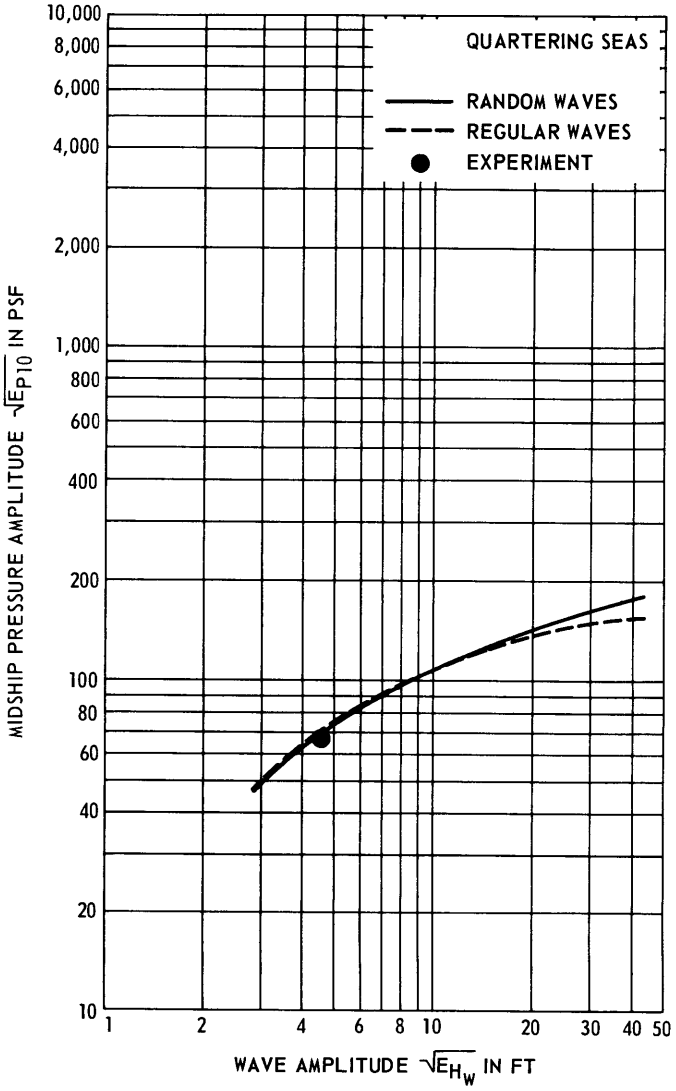

Figure 65 - Midship Pressure Prediction

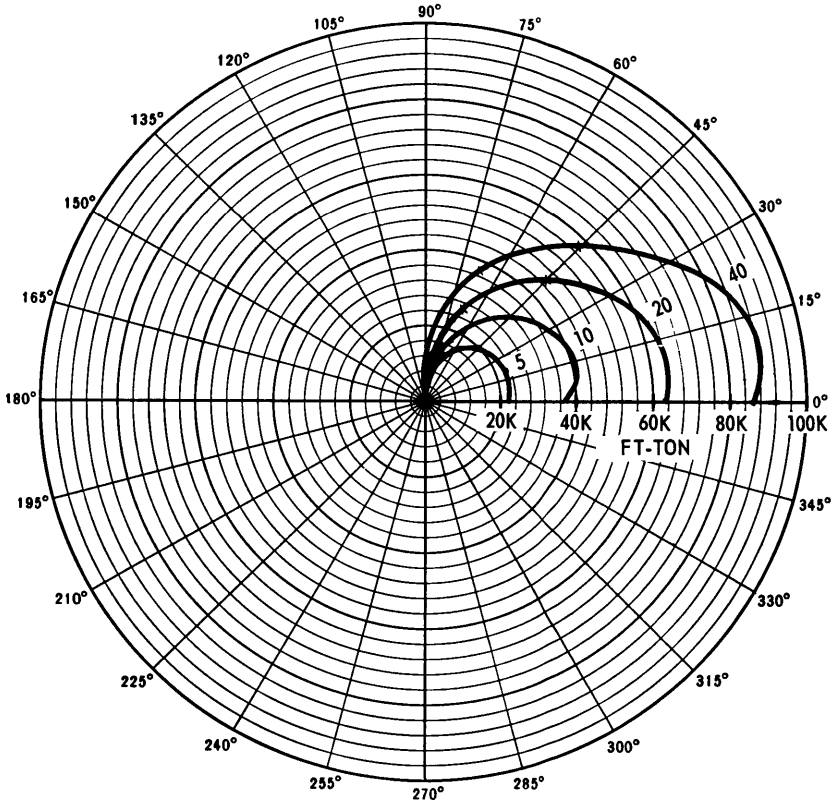

Figure 66 - Midship Vertical Bending Moment Response as a Function of Ship Heading

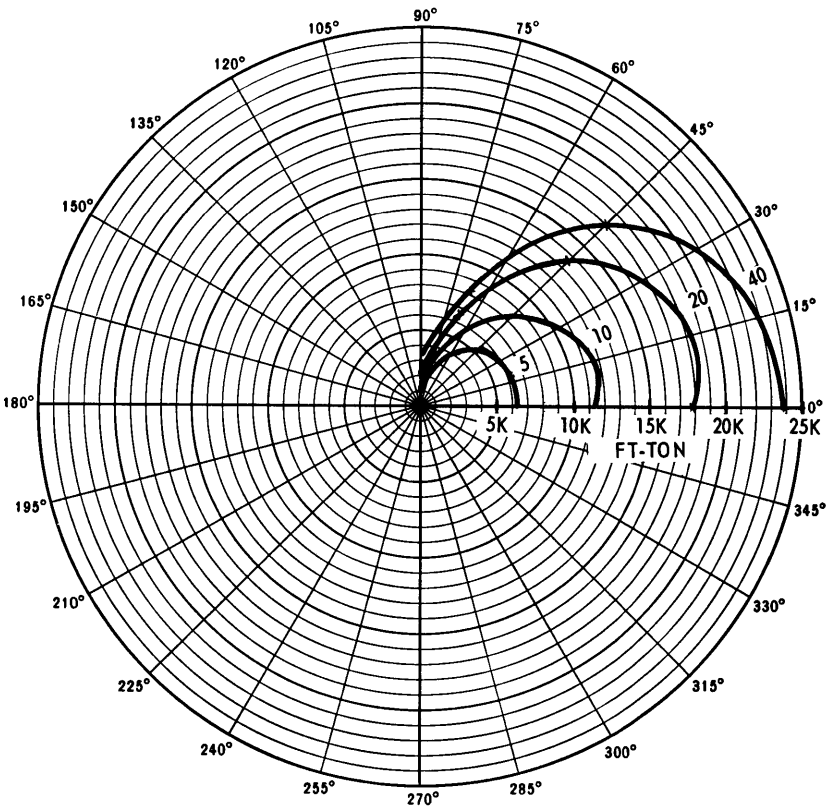

Figure 67 - Station 5 Vertical Bending Moment Response as a Function of Ship Heading

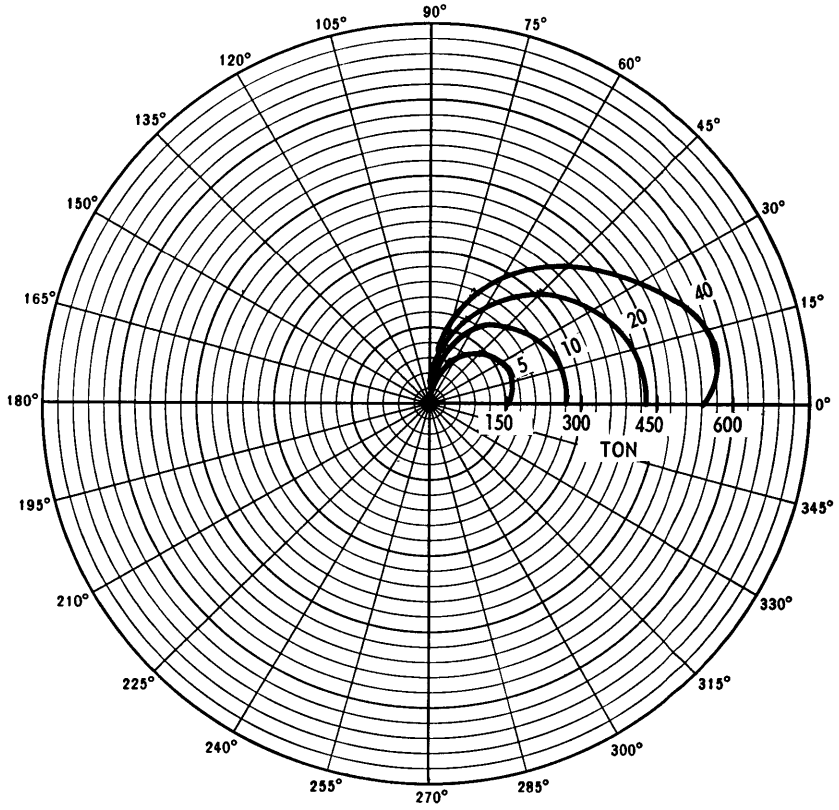

Figure 68 - Station 5 Vertical Shear Response as a Function of Ship Heading

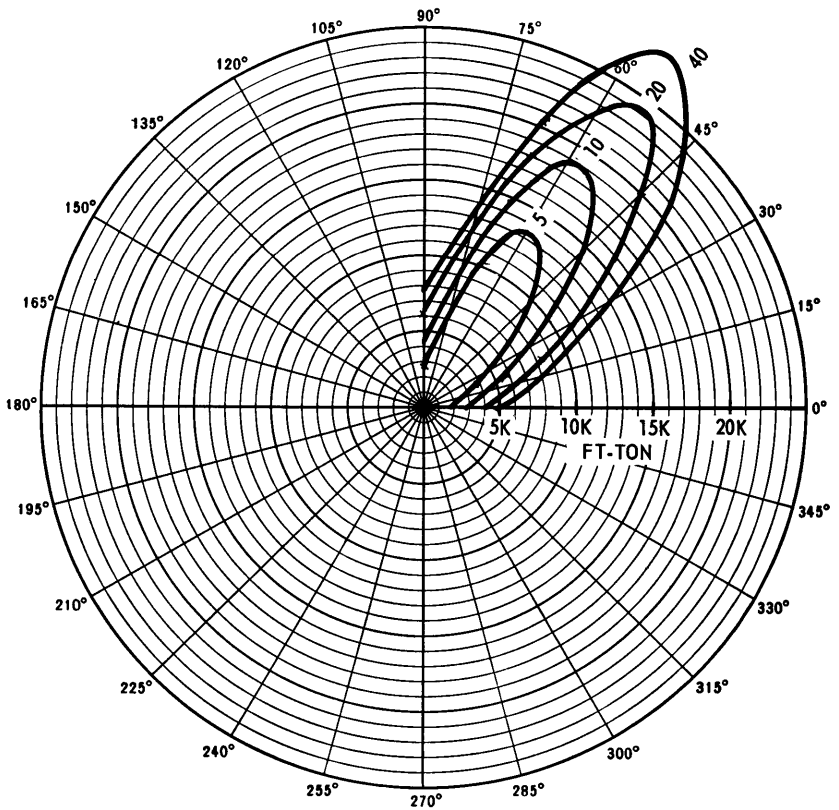

Figure 69 - Midship Transverse Bending Moment Response as a Function of Ship Heading

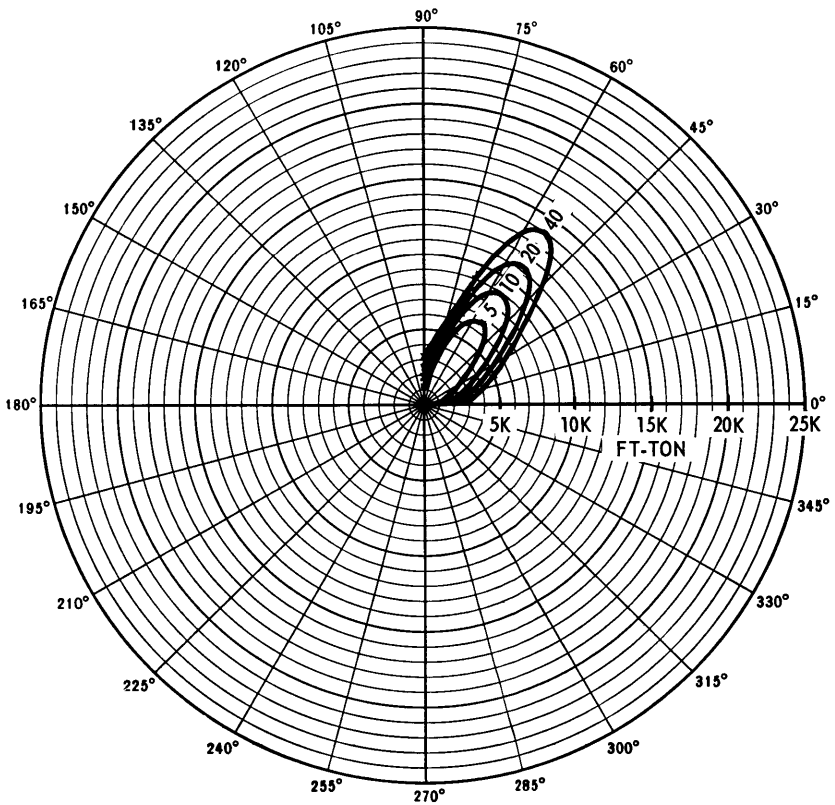

Figure 70 - Station 5 Transverse Bending Moment Response as a Function of Ship Heading

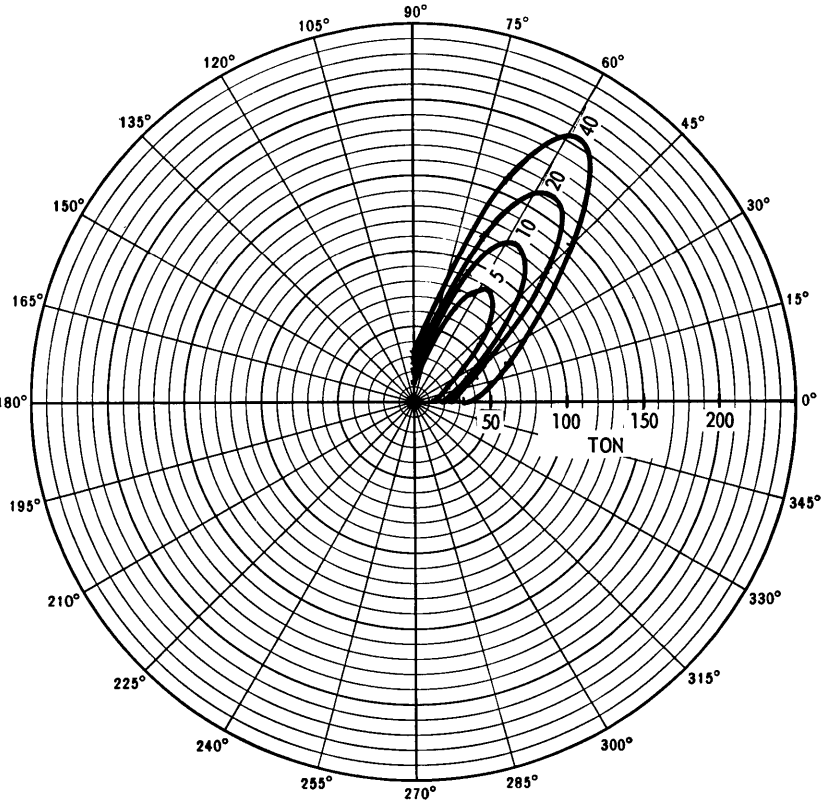

Figure 71 - Station 5 Transverse Shear Response as a Function of Ship Heading

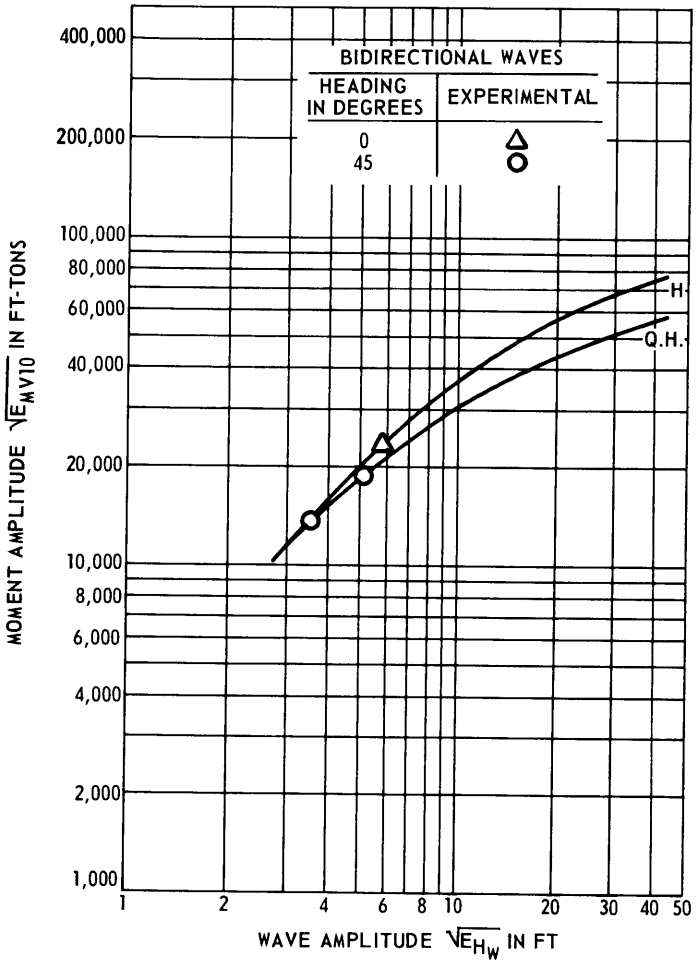

Figure 72 - Midship Vertical Moment Prediction

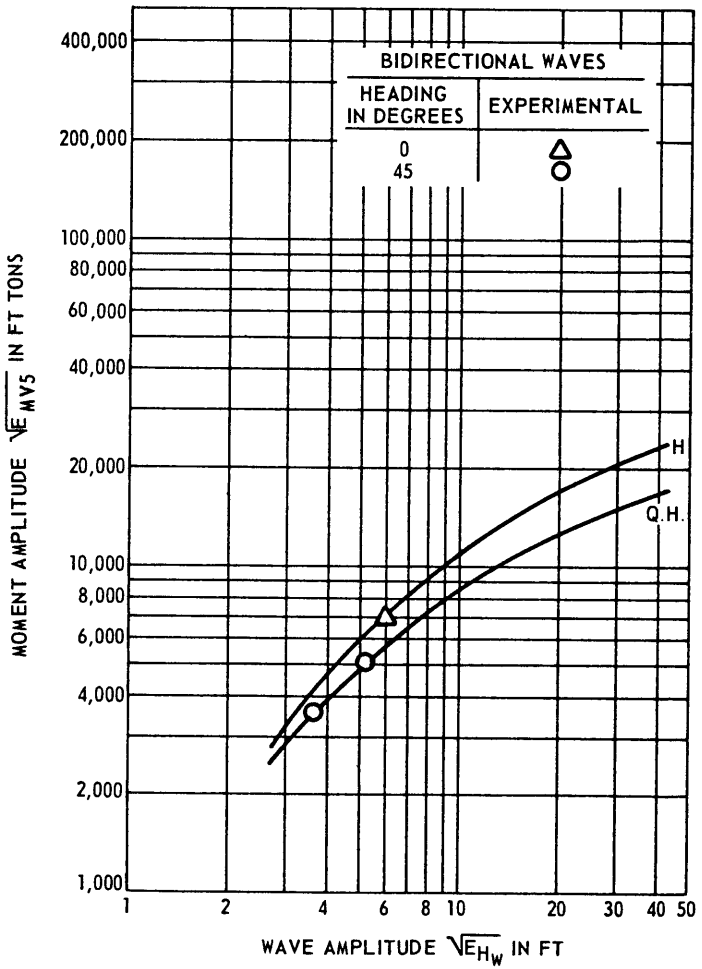

Figure 73 - Station 5 Vertical Moment Prediction

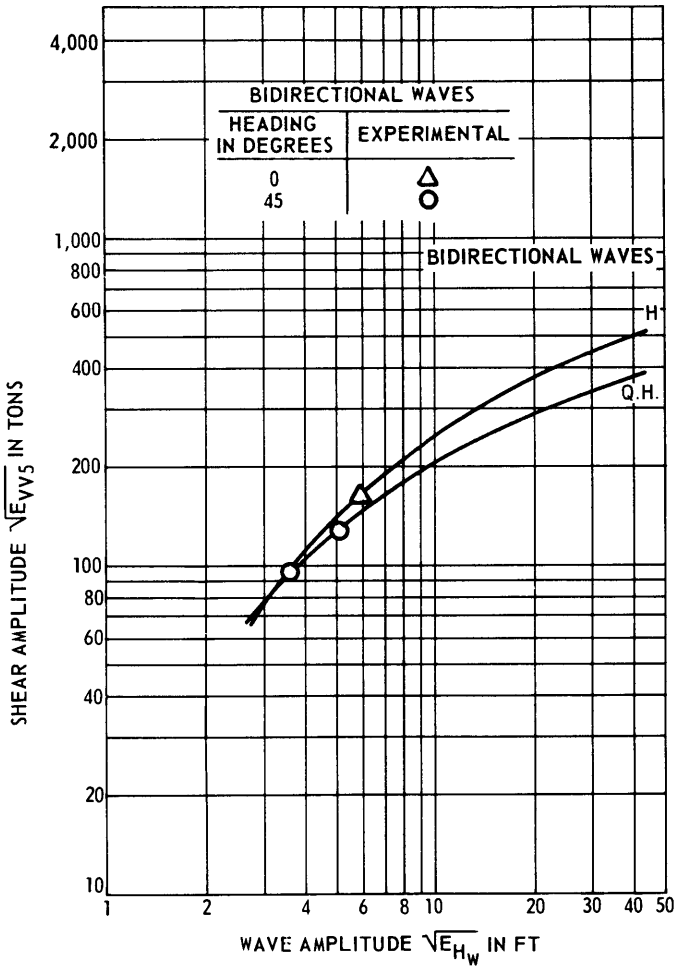

Figure 74 - Station 5 Vertical Shear Prediction

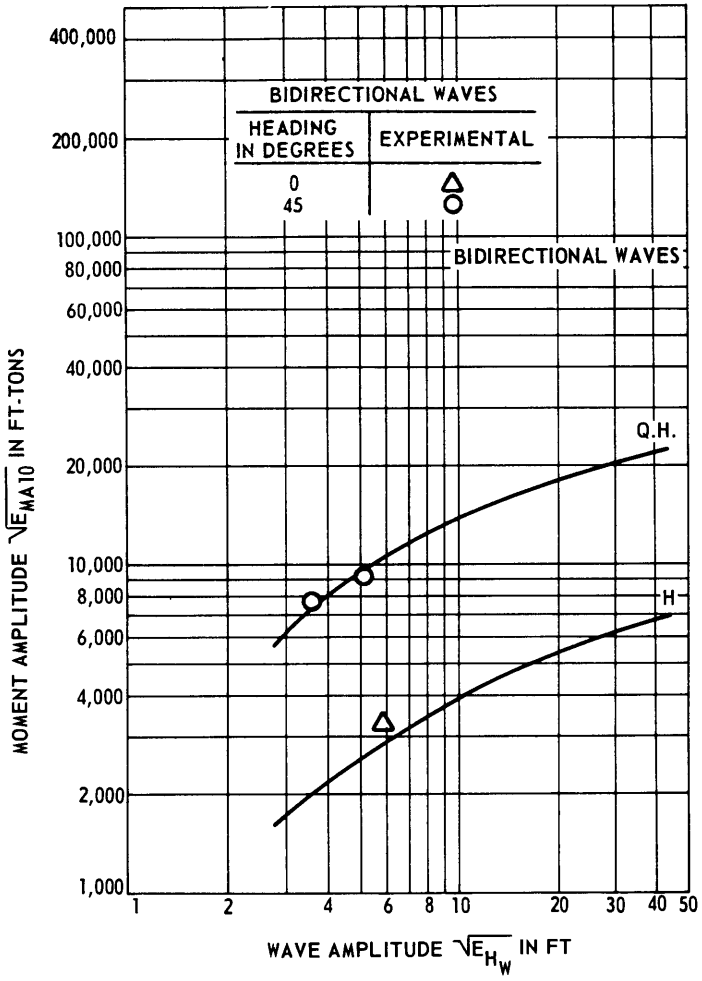

Figure 75 - Midship Transverse Moment Prediction

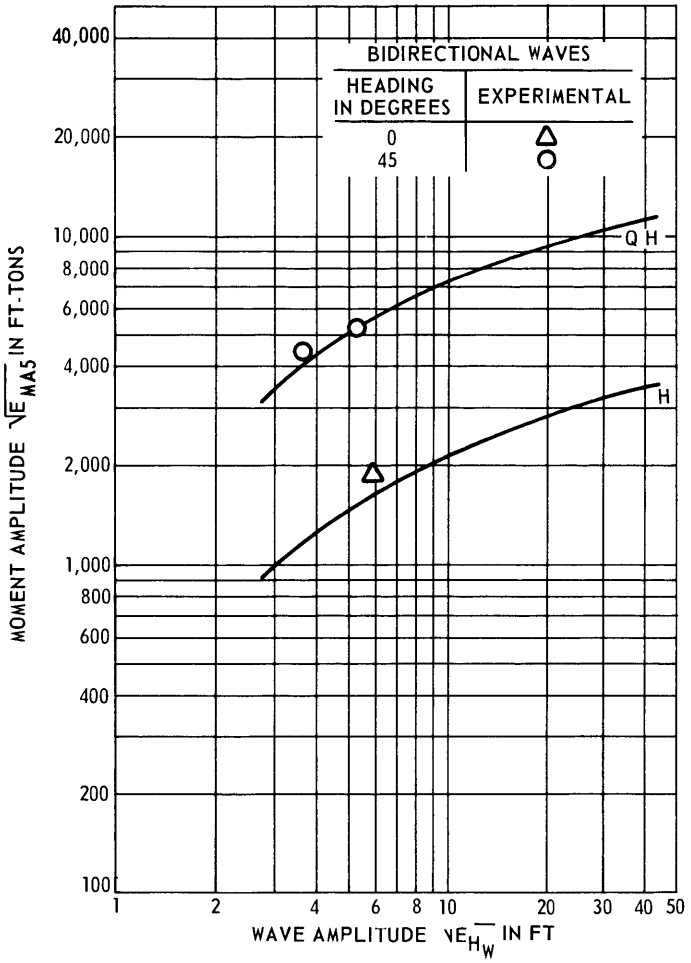

Figure 76 - Station 5 Transverse Moment Prediction

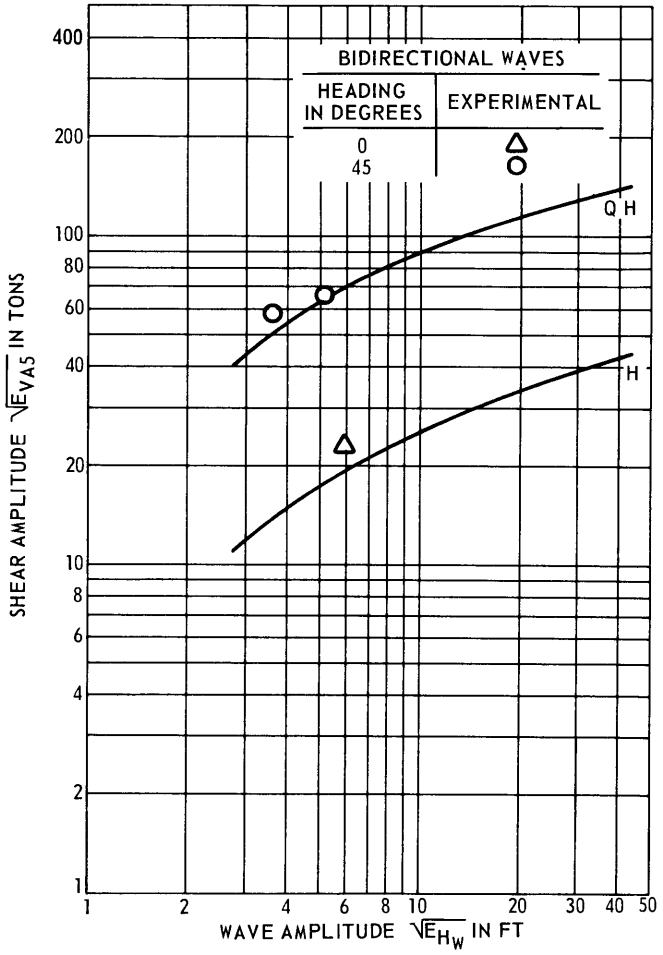

Figure 77 - Station 5 Transverse Shear Prediction

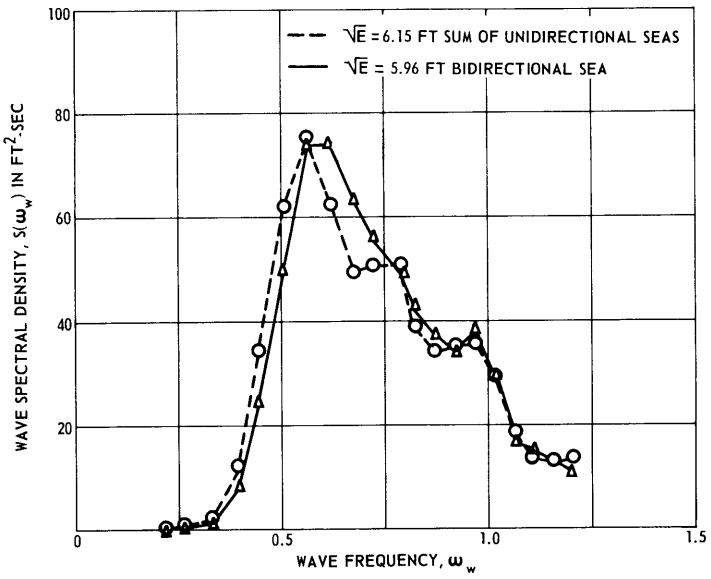

Figure 78 - Comparison of Superposition of Two Unidirectional Seas with a Bidirectional Sea

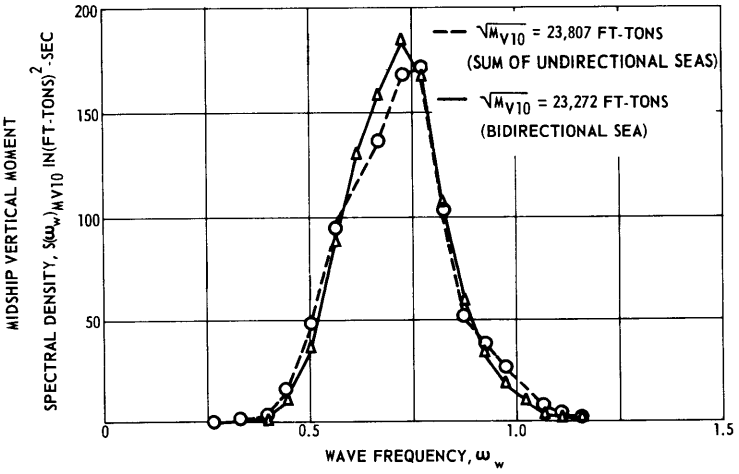

Figure 79 - Comparison of Superposition of Response to Two Unidirectional Seas with Response to a Bidirectional Sea

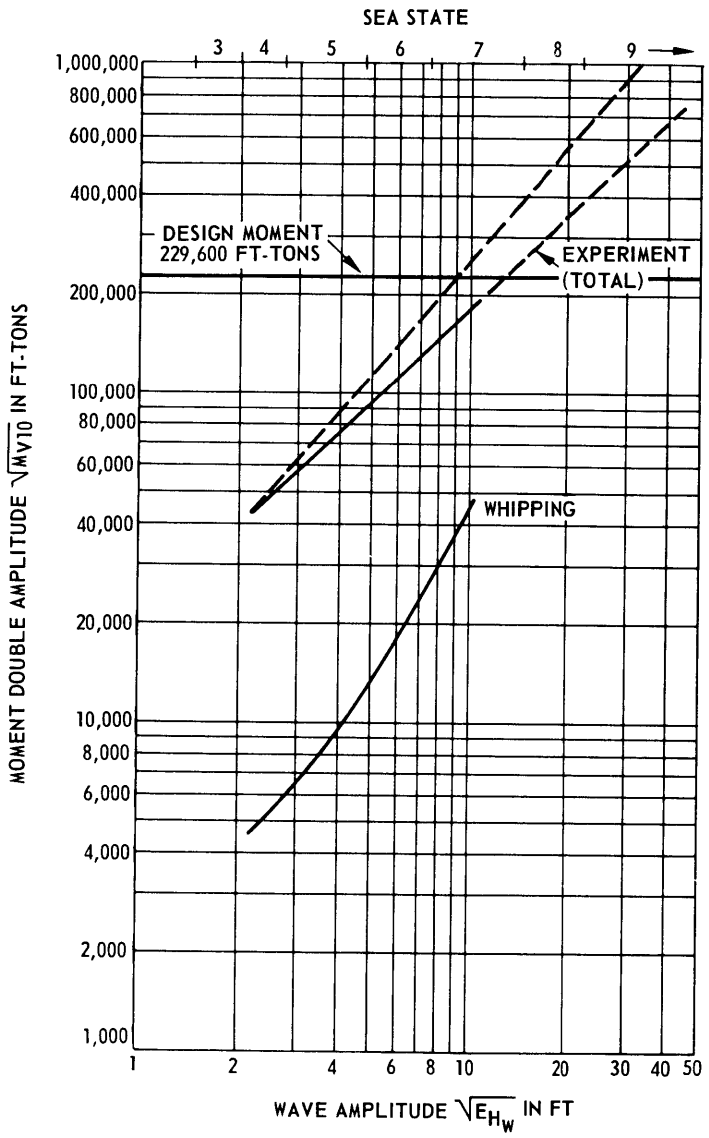

Figure 80 - Maximum Midship Vertical Moment Prediction

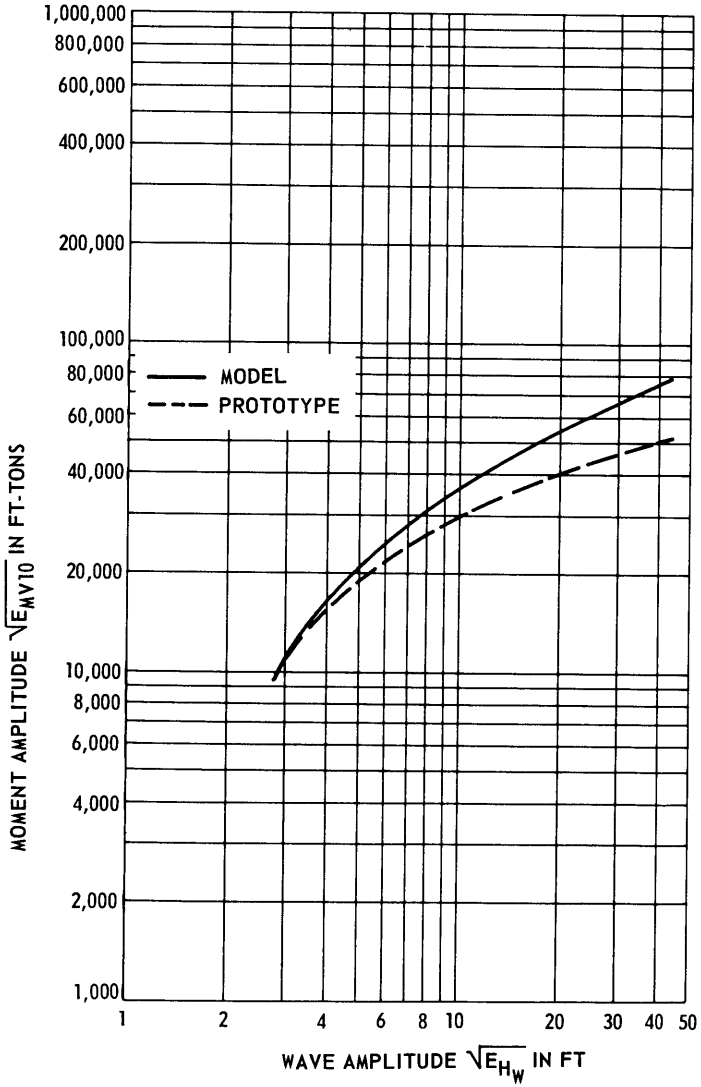

Figure 81 - Comparison of Prototype and Model Midship Vertical Moment, Heading Zero

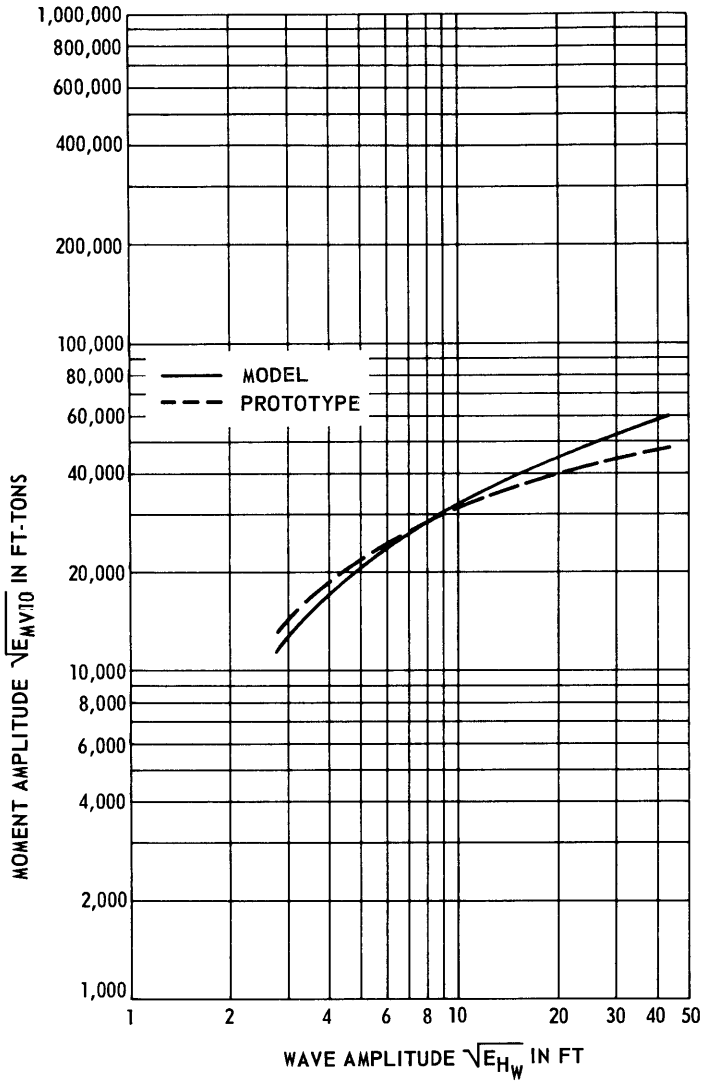

Figure 82 - Comparison of Prototype and Model Midship Vertical Moment, Heading 45 Degrees

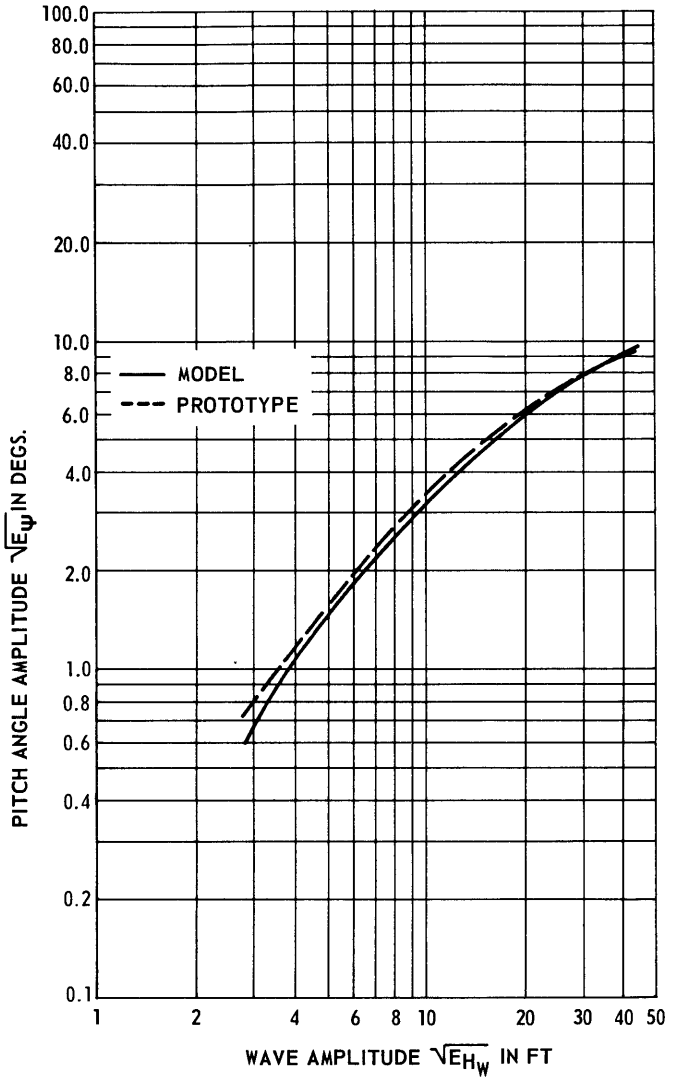

Figure 83 - Comparison of Prototype and Model Pitch Angle, Heading Zero

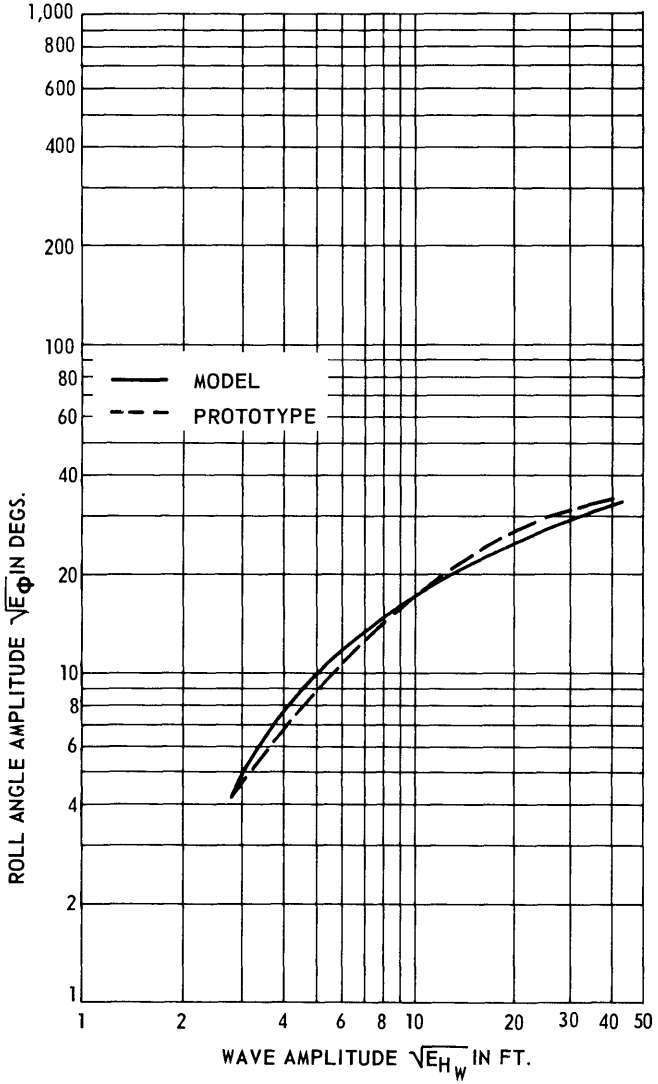

Figure 84 - Comparison of Prototype and Model Roll Angle, Heading 90 Degrees

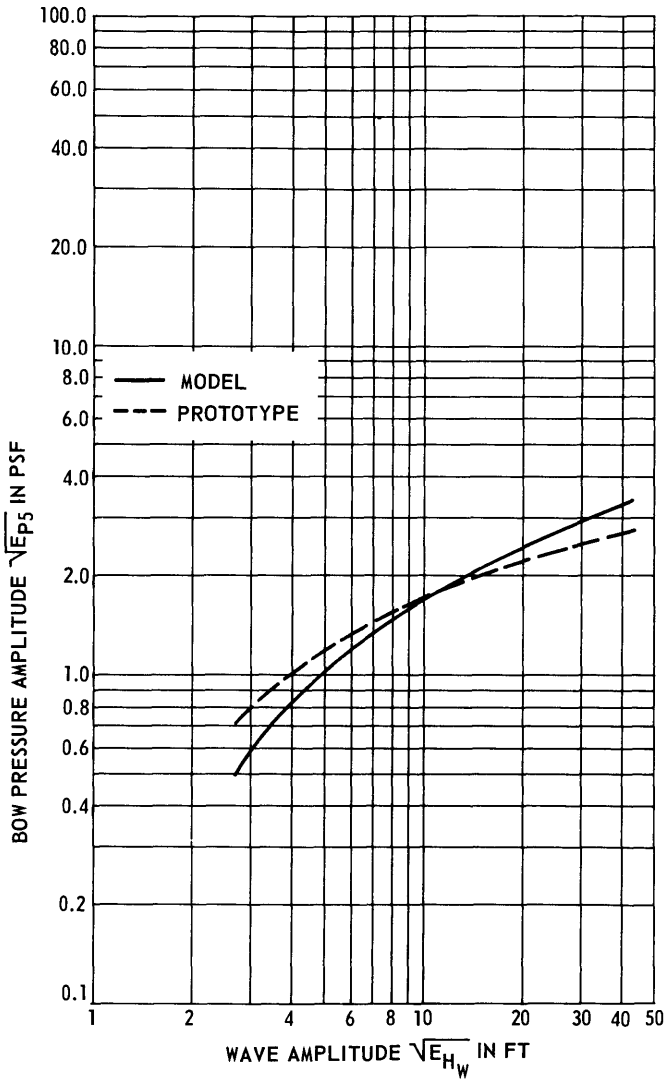

Figure 85 - Comparison of Prototype and Model Bow Pressure, Heading Zero

TABLE 1

Weight Distribution and Strength Properties of DL-2 Destroyer

Station or Section	Section Weight tons	Station Vertical Area Moment of Inertia $in.^2\text{-}ft^2$	Location of Neutral Axis		Station Transverse Area Moment of Inertia $in.^2\text{-}ft^2$	Station Transverse Section Modulus $in.^2\text{-}ft$
			From Keel ft	From Deck ft		
0(FP)						
1	41+70(Dome)					
2	83+60(Dome)					
3	95	121,700	20.7	17.2	86,000	4,700
4	205	136,700	21.0	15.2	146,000	7,200
5	219	152,800	18.9	15.9	202,000	9,300
6	189	176,500	16.9	16.7	253,000	11,200
7	324	187,300	16.1	16.2	278,000	11,900
8	370	203,200	15.5	15.7	312,000	13,200
9	322	182,600	14.4	15.7	364,000	14,800
10	301	189,800	14.6	14.7	374,000	15,100
11	377	181,900	14.1	14.4	373,000	14,900
12	287	168,000	14.0	14.0	385,000	15,300
13	275	156,200	14.4	13.0	352,000	14,100
14	311	127,400	14.1	13.0	297,000	12,000
15	276	104,700	14.1	12.7	265,000	11,000
16	264	69,200	11.8	11.3	212,000	9,100
17	213	39,800	10.2	10.8	157,000	7,000
18	151					
19	134					
20(AP)	108					
	4545 Displacement to DWL					
	130 Dome					
	4675 Total					

TABLE 2

Schedule of Model Tests

Case	Unidirectional Random Waves	
	Heading	Sea State
1	H	4, 6, 7
2	22.5 deg	6
3	Q.H.	4, 5
4	67.5 deg	6
5	B	5
	Bidirectional Random Waves	
6	H	6/6*
7	Q.H.	6/6, 4/6

Note: All tests reported here are for a ship speed of 5 knots. The headings are defined as follows:

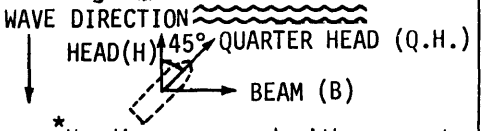

*Heading measured with respect to first sea state number which was generated by the west bank; the two wave generating banks are 90 degrees apart.

TABLE 3

RMS Structural Response from Spectra

All values are given in terms of single amplitudes.

Heading deg	Sea State	Wave Amplitude E_{H_w} ft	Vertical Moment Station 10 $E_{M_{v10}}$ ft-tons	Vertical Moment Station 5 $E_{M_{v5}}$ ft-tons	Vertical Shear Station 5 $E_{V_{v5}}$ tons	Athwartship Moment Station 10 $E_{M_{A10}}$ ft-tons	Athwartship Moment Station 5 $E_{M_{A5}}$ ft-tons	Athwartship Shear Station 5 $E_{V_{A5}}$ tons
0	4	2.20	8,993	2,391	64.0	876	547	6.9
	6	5.49	23,672	6,839	154.1	1,665	1,012	12.2
	7	10.26	33,931	10,963	227.5	2,235	1,290	16.4
	6/6	5.96	23,272	6,991	161.9	3,301	1,891	22.8
22.5	6	5.15	24,905	6,686	163.9	4,533	2,400	31.8
45	4	2.03	8,866	2,223	62.2	5,525	3,065	39.1
	5	4.59	19,622	5,557	126.6	12,236	4,835	75.2
	4/6	3.61	13,447	3,321	95.26	7,854	4,534	58.1
	6/6	5.18	18,593	5,012	126.4	9,194	5,190	65.7
67.5	6	4.63	27,825	4,356	183.9	7,924	3,719	32.3
90	5	2.78	2,537	1,033	17.9	3,696	1,298	19.7

TABLE 4

Maximum Structural Response Recorded from Data

Heading deg	Sea State	Wave Amplitude* $\sqrt{E_{H_w}}$ ft	Vertical Moment Station 10 M_{v10}** ft-tons		Vertical Moment Station 5 M_{v5} ft-tons		Vertical Shear Station 5 V_{v5} tons		Athwartship Moment Station 10 M_{A10} ft-tons		Athwartship Moment Station 5 M_{A5} ft-tons		Athwartship Shear Station 5 V_{A5} tons	
			Wave Induced	Whipping	Wave Induced	Whipping	Wave Induced	Whipping	Wave Induced	Whipping	Wave Induced	Whipping	Wave Induced	Whipping
0	4	2.20	37,731	4,528	10,648	1,610	330	32.7	3,412	2,558	4,398	4,445	35.4	22.3
	6	5.49	85,838	15,092	32,438	6,191	610	107	5,464	3,837	8,610	8,984	59.6	44.7
	7	10.26	138,661	47,163	55,715	24,762	982	315	7,092	14,242	11,230	24,425	77.6	155
	6/6	5.96	98,855	16,602	38,133	6,686	699	101	18,482	14,037	13,369	7,993	124	85.4
22.5	6	5.15	99,043	16,979	30,705	4,952	686	101	15,441	9,358	14,387	5,232	135	57.4
45	4	2.03	45,277	3,773	5,943	842	330	20.1	45,152	8,890	24,705	4,941	261	62.1
	5	4.59	89,611	12,263	30,952	5,200	629	81.8	51,938	15,441	28,484	12,789	310	112
	4/6	3.613	62,634	6,790	18,324	2,971	458	45.3	51,470	7,954	29,646	3,488	363	49.7
	6/6	5.18	89,611	16,035	33,924	5,448	648	88.1	46,323	14,505	34,587	7,848	381	83.8
67.5	6	4.63	50,182	6,792	15,105	3,467	33.7	47.8	37,666	7,954	22,234	4,941	26.4	52.8
90	5	2.78	16,319	7,358	7,874	3,764	84.3	47.8	17,312	8,890	8,662	5,058	113	59.0

*Values are given in terms of single amplitudes.

**Values are given in terms of double amplitudes.

Note: The log-decrement for the model was calculated to be 0.034 as obtained from the whipping response of the midship vertical bending moment measurement.

REFERENCES

1. Dinsenbacher, A.L. and Andrews, J.N., "Vertical and Transverse Load and Motions of a Segmented Model in Regular Waves," NSRDC Report 3152 (Aug 1969).

2. Andrews, J.N. and Dinsenbacher, A.L., "Structural Response of a Carrier Model in Regular and Random Waves," David Taylor Model Basin Report 2177 (Apr 1966).

3. Pierson, Jr., Willard, J. et al., "Observing and Forecasting Ocean Waves by Means of Wave Spectra and Statistics," U.S. Navy Hydrographic Office Publication 603 (1955).

4. Andrews, J.N. and Dinsenbacher, A.L., "Response Amplitude Operators and Whipping Response of a Carrier Model in Random Waves," NSRDC Report 2522 (Jan 1968).

5. Andrews, J.N. and Dinsenbacher, A.L., "Evaluation of Effect of Bow Form on Model Wave-Induced and Whipping Responses," NSRDC Report 2556 (Feb 1968).

6. Andrews, J.N., "Structural Responses and Motions of USS WILLIS A. LEE (DL-4)," NSRDC Report 2997 (Mar 1969).

7. Waterman, R.L. and Clark, D.J., "Structural Test of Bow Sonar Dome and Adjacent Plating on USS WILKINSON (DL-5)," David Taylor Model Basin Report 2036 (Sep 1965).

INITIAL DISTRIBUTION

Copies	
4	NAVSHIPSYSCOM 2 SHIPS 2052 1 SHIPS 031 1 SHIPS 0432
8	NAVSEC 1 SEC 6110 1 SEC 6115 1 SEC 6120 1 SEC 6132 1 SEC 6139 1 SEC 6137 1 SEC 6101 1 SEC 6102C
1	ONR (Code 459)
2	NAVMAT 1 MAT 0331 1 MAT 033A
1	NRL
1	NOL (Code 730)
1	NAVORDSYSCOM (ORD 913)
1	NAVFACENGCOM
2	CDR, NWC, China Lake 1 Code 556 1 Code 5056
1	CNO (Op 07T)
1	USL
1	NASL
1	NELC
1	DNL
1	COMCRUDESLANT
1	COMCRUDESPAC
1	NAVSHIPYD BSN
1	NAVSHIPYD LBEACH
1	NAVSHIPYD NORVA
1	COGARD Attn: Testing & Dev Div
1	Nat'l Sci Foundation

Copies	
1	MARAD Attn: Div of Ship Design
2	Nat'l Research Council 1 Mr. A.R. Lytle 1 Ship Struct. Comm
1	SNAME, New York
20	DDC
1	MIT Attn: Dr. A.H. Keil
1	Lehigh Univ Attn: Dept of Mechanics
1	Supt, USNPGSCHOL, Monterey
1	Univ of Calif Attn: Dept Naval Architecture
2	Southwest Research Inst 1 Dr. R. DeHart 1 Dr. H.N. Abramson
1	Webb Institute Attn: Prof Maclean
1	Univ of Michigan Attn: Dept Engr Mechanics
1	SIT, DL

☆ U.S. GOVERNMENT PRINTING OFFICE: 1970-397-175/66

UNCLASSIFIED

Security Classification

DOCUMENT CONTROL DATA - R & D

(Security classification of title, body of abstract and indexing annotation must be entered when the overall report is classified)

1 ORIGINATING ACTIVITY (Corporate author)	2a. REPORT SECURITY CLASSIFICATION
Naval Ship Research and Development Center Washington, D.C. 20007	UNCLASSIFIED
	2b. GROUP 2

3 REPORT TITLE

MODEL AND PROTOTYPE RESPONSES FOR A DL CLASS DESTROYER

4 DESCRIPTIVE NOTES (Type of report and inclusive dates)

Final

5 AUTHOR(S) (First name, middle initial, last name)

John N. Andrews

6 REPORT DATE	7a. TOTAL NO OF PAGES	7b. NO OF REFS
March 1970	62	7

8a. CONTRACT OR GRANT NO	9a. ORIGINATOR'S REPORT NUMBER(S)
b. PROJECT NO SF 35 422 301	3325
c. Task 1973	9b. OTHER REPORT NO(S) (Any other numbers that may be assigned this report)
d.	

10. DISTRIBUTION STATEMENT

This document is subject to special export controls and each transmittal to foreign governments or foreign nationals may be made only with prior approval of Naval Ship Research and Development Center, Code 700.

11 SUPPLEMENTARY NOTES	12 SPONSORING MILITARY ACTIVITY
	NAVSHIPS

13 ABSTRACT

This report presents test results for a segmented structural model of the DL-2-Class destroyer in random waves (unidirectional and bidirectional) together with regular wave results derived from earlier tests. Vertical and transverse bending moments were measured at two longitudinal positions on the model. Vertical and transverse shear forces were measured at the quarter-point. Motion measurements (pitch angle, roll angle, bow acceleration, and heave displacement) were made as were pressures at two positions along the keel.

Response amplitude operators (RAOs) derived from regular and random wave tests are compared. Neumann sea spectra, together with RAOs, are utilized to obtain prediction curves of ship response. Maximum whipping response for the vertical midship bending moment is augmented with the maximum wave-induced response and compared with the conventional design midship bending moment. The spectra for two unidirectional seas whose directions are 90 deg apart were combined and compared with the corresponding bidirectional sea. The same procedure was applied to the corresponding midship vertical bending moment response.

Comparison of model and prototype test results are made by means of prediction curves.

14 KEY WORDS	LINK A		LINK B		LINK C	
	ROLE	WT	ROLE	WT	ROLE	WT
Surface Ship						
Response						
Model Testing						